

LIBRARY

The

# Marconi Review

122

3rd QUARTER 1956

Vol. XIX

**CONTENTS:**

V.H.F. Band II Harmonic Filter	- - - - -	89
The Use of a Horizontal Dipole as a Direction Finding Aerial	-	97
Wide-angle Scanning Performance of Mirror Aerials	- - -	119

# THE MARCONI GROUP OF COMPANIES IN GREAT BRITAIN

---

Registered Office : Marconi House,  
Strand,  
London, W.C.2.  
Telephone : Covent Garden 1234.

---

## MARCONI'S WIRELESS TELEGRAPH COMPANY, LIMITED

Marconi House,  
Chelmsford,  
Essex.

Telephone : Chelmsford 3221.  
Telegrams : Expanse, Chelmsford.

## THE MARCONI INTERNATIONAL MARINE COMMUNICATION COMPANY, LIMITED

Marconi House,  
Chelmsford,  
Essex.

Telephone : Chelmsford 3221.  
Telegrams : Thulium, Chelmsford.

## THE MARCONI SOUNDING DEVICE COMPANY, LIMITED

Marconi House,  
Chelmsford,  
Essex.

Telephone : Chelmsford 3221.  
Telegrams : Thulium, Chelmsford.

## THE RADIO COMMUNICATION COMPANY, LIMITED

Marconi House,  
Chelmsford,  
Essex;

Telephone : Chelmsford 3221.  
Telegrams : Thulium, Chelmsford

## THE MARCONI INTERNATIONAL CODE COMPANY, LIMITED

Marconi House,  
Strand,  
London, W.C.2.

Telephone : Covent Garden 1234.  
Telegrams : Docinocram.

## MARCONI INSTRUMENTS, LIMITED

St. Albans,  
Hertfordshire.

Telephone : St. Albans 6161/5.  
Telegrams : Measurtest, St. Albans.

## SCANNERS LIMITED

Woodskippers Yard,  
Bill Quay,  
Gateshead, 10,  
Co. Durham.

Telephone : Felling 82178.  
Telegrams : Scanners, Newcastle-upon-Tyne.

# THE MARCONI REVIEW

---

No. 122

Vol. XIX

3rd Quarter, 1956

---

---

Editor : L. E. Q. WALKER, A.R.C.S.

The copyright of all articles appearing in this issue is reserved by the 'Marconi Review.' Application for permission to reproduce them in whole or in part should be made to Marconi's Wireless Telegraph Company Ltd.

---

---

## V.H.F.—BAND II HARMONIC FILTER

BY B. M. SOSIN, B.Sc., A.M.I.E.E.

*The following article describes a design procedure for a harmonic filter to be used on Band II broadcast transmitters. A particular type of filter economically constructed from transmission line elements is designed to give a prescribed insertion loss.*

### Introduction

WITH the increasing use of V.H.F. and U.H.F. for television and communication, harmonic filters for V.H.F. Band II broadcast transmitters have become necessary. A harmonic content as low as 25 mW is often required and the filter must handle the full power output of the transmitter. Because of this such a filter has to be constructed from lengths of transmission lines and unless very carefully designed its cost can add considerably to the cost of the transmitter. With this in view, the minimum required insertion loss of the filter was deduced and a varying impedance type filter<sup>(1,2)</sup> was chosen as this offered the simplest mechanical structure. This was analysed and designed to the prescribed requirements. The resultant filter, whilst fully satisfactory, cost only one-eighth the manufacturing cost of the filter it replaces. The original filter had been designed by the classical method and contained one constant-k section and two m-derived half sections constructed with transmission line elements.

### Insertion Loss Requirements

The total harmonic content was specified to be less than 25 mW, i.e. —56 db of 10 kW transmitted power. The harmonic output of the transmitter was taken as about —40 db (for second or third harmonics), but it does not follow that in the harmonic filter an insertion loss of only 16 db is required, as there may be a build-up in the feeder line joining the transmitter and the filter.

The problem is best treated by wave equations. (See appendix.) Consider

Fig. 1 in which the transmitter is connected to the load through a length of transmission line of an electrical length  $\theta$  and a harmonic filter. The harmonic wave  $I_p$  (conveniently referred to full power of the transmitter) is attenuated in the trans-



FIG. 1  
General arrangement.

mitter, by an amount  $T_T$ , taken as  $-40$  db, and is directed towards the filter. The wave  $I_2$  is the incident wave on the filter and, after being partially reflected (shown as wave  $R_2$ ), will arrive back to the transmitter, where it will again be partially reflected and will add to the wave  $R_1$ .  $K_T$  and  $K_{F2}$  are the reflection coefficients of the transmitter and filter respectively. The wave  $I_2$  will also pass through the filter and will be attenuated by an amount  $T_F$ .  $R_3$  is the wave travelling from the filter to the load and  $I_3$  the wave reflected from the load. The last will be sufficiently small to be neglected.

The wave matrix (see appendix) becomes,

$$\begin{vmatrix} R_1 \\ I_1 \end{vmatrix} = \begin{vmatrix} e^{j\theta} & 0 \\ 0 & e^{-j\theta} \end{vmatrix} \begin{vmatrix} \frac{1}{T_F} & -\frac{K_{F3}}{T_F} \\ \frac{K_{F2}}{T_F} & T_F - \frac{K_{F2}K_{F3}}{T_F} \end{vmatrix} \begin{vmatrix} R_3 \\ I_3 (=0) \end{vmatrix}$$

and 
$$R_1 = T_T I_p + K_T I_1$$

which will reduce to

$$\frac{R_3}{I_p} = T = \frac{T_T T_F}{e^{j\theta} (1 - K_T K_{F2} e^{-j2\theta})} \tag{1}$$

Hence

$$|T| = \frac{T_T T_F}{\sqrt{1 + |K_T K_{F2}|^2 - 2|K_T K_{F2}| \cos \theta_{tot}}} \tag{2}$$

in which  $\theta_{tot}$  is the total phase angle including that of the reflection coefficients.

If  $|K_T K_{F2}|$  is small, i.e. if the harmonic filter is of the absorptive type or if fairly high dissipative losses are present at the filter and at the transmitter, the denominator of equation (2) approaches unity. Hence

$$|T| \doteq |T_T \times T_F|$$

i.e. the insertion loss of the filter in db can be added to the attenuation of harmonics in the transmitter to obtain the final harmonic content.

In practice, however, the filter is of the reflective type, and its reflection coefficient will be of the order of 0.98. The reflection coefficient of the transmitter is difficult to estimate and almost impossible to measure, but because of a fair amount of dissipation present in the circuits, it should not be more than 0.90.

Hence, taking

$$\begin{aligned} |T_T| &= -40 \text{ db} \\ |K_T| &= 0.90 \\ |K_{F2}| &= 0.98 \end{aligned}$$

the value of  $|T_F|$  must be such that for any angle  $\theta_{tot}$  (this angle is unknown, and depends on installation, tuning of the transmitter and the filter itself)  $|T|$  must be less than  $-56$  db.

Hence from equation (2)

$$|T_F| = \frac{|T|}{|T_T|} \times \{1 - |K_T K_F|\} \doteq -35 \text{ db}$$

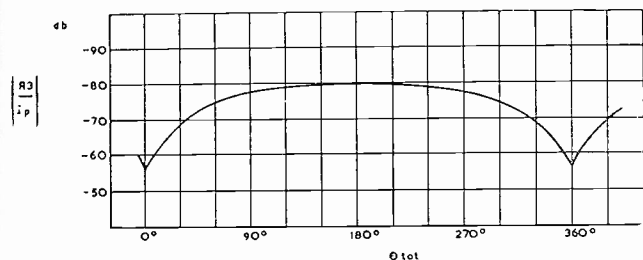


FIG. 2

Harmonic content as a junction of total loop phase angle between the transmitter and the filter taking:

$$T_T = -40 \text{ db}, T_F = -35 \text{ db}, K_{T+} = 0.90, K_{F2} = 0.98.$$

Fig. 2 shows clearly that under most conditions the harmonic content will be very much smaller than the maximum value of  $-56$  db.

### Type of Filter

The harmonic filter comes under the general classification of low pass filters, i.e. it will have a pass band up to above the working band of frequencies and a

high attenuation above the transition band. Such a filter imposes fairly severe limitations on design which are entirely unjustified. In the present design, although still in principle a low pass filter, limitations were relaxed by selecting elements in such a way as to obtain correct impedance matching over the working frequency band without consideration of what happens above and below and by making the maximum attenuation in the second and third harmonic region with gradual reduction above these frequencies (this reduction is unavoidable for any filter composed of distributed parameter elements).

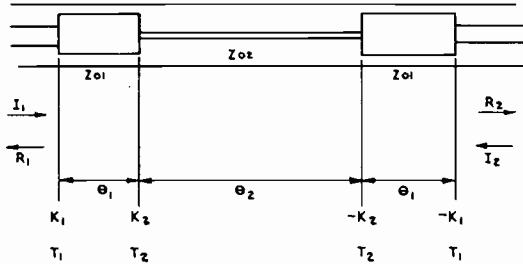
Considering the high power to be transmitted at Band II V.H.F., the only realizable elements of the filter will be of the distributed parameter type, i.e. the filter will be constructed from sections of transmission lines. The simplest mechanical structure is obtained with a varying impedance type filter<sup>(1, 2)</sup>. Such a filter is in effect a length of transmission line of which the inner conductor is alternately of large and small diameter giving low and high characteristic impedance respectively.

Although mechanically simple, the electrical design presents a difficult mathematical problem if the filter is to be designed to the prescribed insertion loss characteristic as stated above. The lump parameter approximations cannot be used because at the harmonic frequencies the approximation will be far from correct. A section consisting of low, high and low characteristic impedance transmission lines connected in tandem was first analysed by means of a transmission matrix. The equations obtained were unmanageable. A different approach by means of a wave matrix was partly successful, that is, a complete filter is split up into a number of identical sections and each section is designed to the specified performance derived from the performance of a complete filter. Finally, the pass input reflection coefficient curve is centralized. No solution was found for the direct design of a complete filter.

**One Section**

Consider a section as shown in Fig. 3.

If we take  $Z_{01}$  and  $Z_{02}$  as the characteristic impedances of the lines,  $\theta_1$  and  $\theta_2$  as their respective electrical lengths and  $Z_0$  the characteristic impedance of the input and output feeder, then the step reflection and transmission coefficients are:—



$$\begin{aligned}
 K_1 &= \frac{Z_{01} - Z_0}{Z_{01} + Z_0} \\
 T_1 &= \frac{2\sqrt{Z_0 Z_{01}}}{Z_{01} + Z_0} \\
 K_2 &= \frac{Z_{02} - Z_{01}}{Z_{02} + Z_{01}} \\
 T_2 &= \frac{2\sqrt{Z_{01} Z_{02}}}{Z_{02} + Z_{01}}
 \end{aligned} \tag{3}$$

FIG. 3  
One section of the filter.

The input incident and reflected waves  $I_1$  and  $R_1$  are related to the output “reflected” and incident waves  $R_2$  and  $I_2$  by the matrix equation

$$\begin{aligned}
 \begin{pmatrix} I_1 \\ R_1 \end{pmatrix} &= \frac{1}{T_1^2 T_2^2} \begin{pmatrix} 1 & K_1 \\ K_1 & 1 \end{pmatrix} \begin{pmatrix} e^{j\theta_1} & 0 \\ 0 & e^{-j\theta_1} \end{pmatrix} \begin{pmatrix} 1 & K_2 \\ K_2 & 1 \end{pmatrix} \begin{pmatrix} e^{j\theta_2} & 0 \\ 0 & e^{-j\theta_2} \end{pmatrix} \begin{pmatrix} R_2 \\ I_2 \end{pmatrix} \\
 &\times \begin{pmatrix} 1 & -K_2 \\ -K_2 & 1 \end{pmatrix} \begin{pmatrix} e^{j\theta_1} & 0 \\ 0 & e^{-j\theta_1} \end{pmatrix} \begin{pmatrix} 1 & -K_1 \\ -K_1 & 1 \end{pmatrix} \begin{pmatrix} R_2 \\ I_2 \end{pmatrix}
 \end{aligned} \tag{4}$$

Hence

$$\frac{K}{T} = \frac{j2}{T_1^2 T_2^2} \{K_1 \sin(2\theta_1 + \theta_2) + K_2(1 + K_1^2) \sin \theta_2 + K_1 K_2^2 \sin(-2\theta_1 + \theta_2)\} \tag{5}$$

where  $K$  is the input reflection coefficient of the section and  $T$  is the transmission coefficient of the section.

In the pass band  $|T|$  tend to unity.

The condition for  $K = 0$  is given by

$$\tan \theta_2 = \frac{-K_1 T_2^2 \sin 2\theta_1}{K_2(1 + K_1^2) + K_1(1 + K_2^2) \cos 2\theta_1} \tag{6}$$

Also from equation (4)

$$\begin{aligned}
 \frac{1}{T} &= \frac{1}{T_1^2 T_2^2} \{T_1^2 [\cos(2\theta_1 + \theta_2) - K_2^2 \cos(-2\theta_1 + \theta_2)] \\
 &+ j[(1 + K_1^2) \sin(2\theta_1 + \theta_2) + 4K_1 K_2 \sin \theta_2 + K_2^2(1 + K_1^2) \sin(-2\theta_1 + \theta_2)]\}
 \end{aligned} \tag{7}$$

Also when  $K = 0$

$$\tan(\arg. T) = \frac{-K_2 T_1^2 \sin 2\theta_1}{K_1(1 + K_2^2) + K_2(1 + K_1^2) \cos 2\theta_1} \tag{8}$$

### Number of Sections

Connecting two sections in tandem we have

$$T_{2\text{tot}} = \frac{T^2}{1 - K^2} \tag{9}$$

$$K_{2\text{tot}} = K \frac{1 + T^2 - K^2}{1 - K^2} = K[1 + T^2(1 + K^2 + K^4 + \dots)] \tag{10}$$

Equation (9) shows clearly how easily an additional pass band or drop in the insertion loss in the stop band is formed simply by the reflection coefficient of the sections becoming real.

Equation (10) shows that by making the phase shift through the section about 90° in the pass band, the overall input reflection coefficient will be reduced (a known fact).

For three sections in tandem

$$T_{3\text{tot}} = \frac{T T_{2\text{tot}}}{1 - K K_{2\text{tot}}} = \frac{T^3}{(1 - K^2)^2 - K^2 T^2} \tag{11}$$

and

$$T_{3\text{tot}} \doteq \frac{T^3}{(1 - K^2)^2} \quad \text{for } T \rightarrow 0$$

$$(1 - K^2) \text{ not } \rightarrow 0$$

Also

$$K_{3\text{tot}} = \frac{K + K_{2\text{tot}}(T^2 - K^2)}{1 - K K_{2\text{tot}}} \tag{12}$$

and

$$K_{3\text{tot}} \doteq K \{ 1 + T^2(1 + K^2 + K^4 \dots) + T^4(1 + 3K^2 + 6K^4 + \dots) + T^6(K^2 + 5K^4 + \dots) + T^8 K^4 + \dots \}$$

In the pass band, i.e. for small reflection coefficients of the section, equation (11) will reduce to

$$K_{3\text{tot}} \doteq K \{ 1 + T^2 + T^4 \} \tag{13}$$

Again the overall input reflection coefficient can be reduced by making the phase shift per section of the order of 60° or 120°.

### Design and Performance

The harmonic filter is used in conjunction with the standard 3½ inch diameter 51.5 ohm coaxial feeder, hence it is desirable, if possible, to use the same outer conductor as that of the feeder. The inner conductor is alternatively of a large and small diameter to give low and high characteristic impedance transmission lines for the filter elements. The power handling capacity sets the limit here. The maximum characteristic impedance of a line is limited by the copper losses and heat dissipation of the inner conductor. The minimum characteristic impedance is limited by the voltage breakdown of the small gap between the inner and outer conductors. Putting polyethylene lining of a suitable thickness into the inside of the outer tube, not only reduces the minimum permissible characteristic impedance, but provides an effective and cheap support for the inner conductor assembly. A large ratio of maximum and minimum characteristic impedances is required in

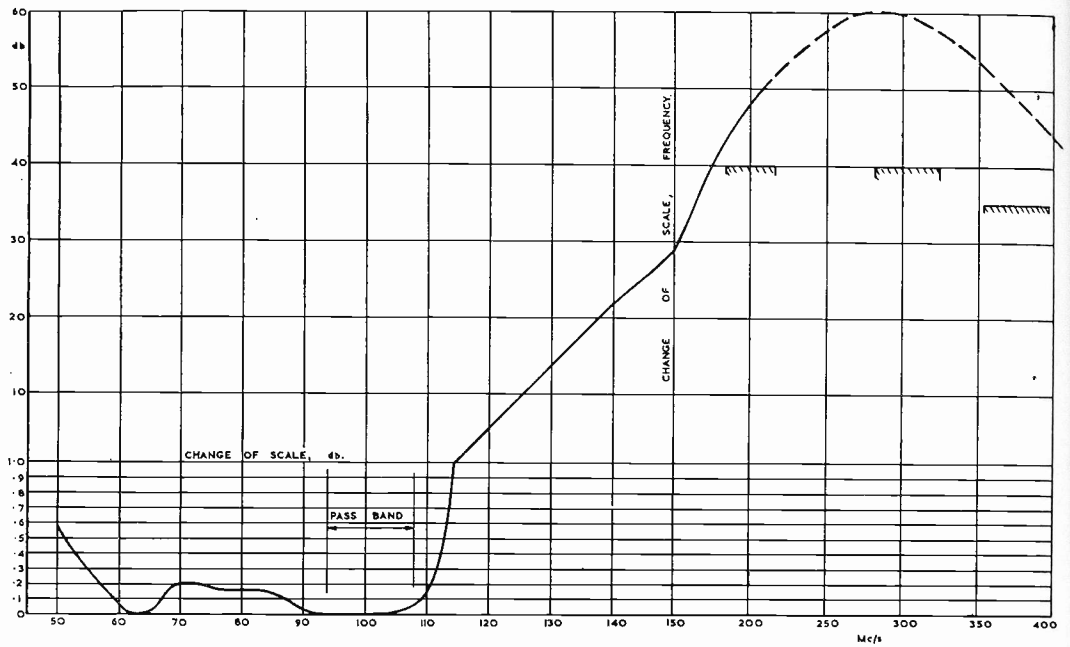


FIG. 4  
*Insertion loss of the harmonic filter.*

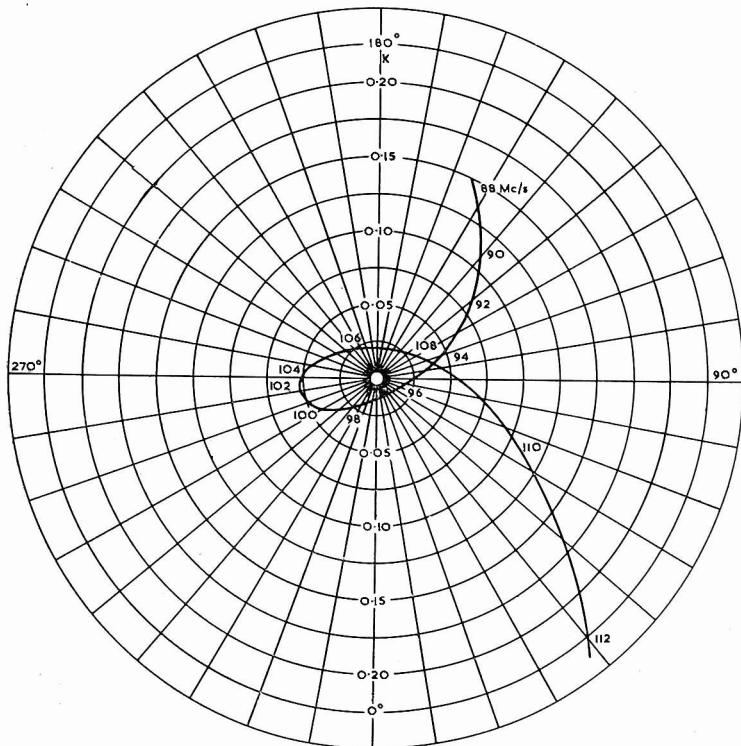


FIG. 5  
*Input Reflection Coefficient.*

order to make the length of a section of the filter short and hence to push the second pass band or "trough," in the stop insertion loss curve, above frequencies of interest. (See equation (7).)

Having decided on the characteristic impedance of the transmission line elements, values of  $\theta_1$  are found from equation (8) which give arguments of  $T$  of  $-60^\circ$ ,  $-90^\circ$ ,  $-120^\circ$  etc., for three, two, three, etc., sections respectively. The corresponding values of  $\theta_2$  are obtained from equation (6). Calculation of the transmission coefficient at harmonic frequencies and of the reflection coefficient at the edges of the pass band for the conditions selected above, and comparison with the required specification gives the number of sections needed. The filter as calculated above will have zero reflection coefficient in the centre of the pass band; at the edges the modulus of the reflection coefficients will be approximately the same and the angles will not differ much. Therefore it will form a loop as plotted on polar co-ordinates. The over-all reflection coefficient can thus be reduced by centralizing the loop. No attempt was made to calculate the necessary changes to the lengths of the filter elements for this purpose, because this is best done during the test.

A filter was designed as described above consisting of three sections taking approximately 3 feet length of the feeder run. From the outside it is practically indistinguishable from the feeder. The performance is entirely satisfactory, as can be clearly seen from Fig. 4 and Fig. 5 giving insertion loss and input reflection coefficient of the filter covering the 94 Mc/s to 108 Mc/s band. A similar filter was designed for the 87.5 Mc/s to 100 Mc/s band.

### APPENDIX

Explanatory note on wave matrix.<sup>(3, 4)</sup>

Consider a two-pair terminal network as shown on Fig. 6 in which

$I_1, I_2$ , are the incident waves

and  $R_1, R_2$ , are the "reflected" waves.



FIG. 6

Two-pair terminal network.

A wave is here defined as the square root of the product of voltage and current existing on a transmission line when the latter is correctly terminated, i.e. the values are normalized to the characteristic impedance of the line. The phase angle is taken as that of the voltage. When the line is not properly terminated two waves exist, a forward wave and a backward wave.

Also  $K_1, K_2$ , are the reflection coefficients of the network and  $T$  is the transmission coefficient.

Then

$$\begin{vmatrix} I_1 \\ R_1 \end{vmatrix} = \begin{vmatrix} \frac{1}{T} & -\frac{K_2}{T} \\ \frac{K_1}{T} & T - \frac{K_1 K_2}{T} \end{vmatrix} \begin{vmatrix} R_2 \\ I_2 \end{vmatrix} \quad (14)$$

Also

$$\begin{vmatrix} 1 & -\frac{K_2}{T} \\ \frac{K_1}{T} & T - \frac{K_1 K_2}{T} \end{vmatrix} = 1$$

and for a lossless network

$$\begin{aligned} |K_1| &= |K_2| \\ |T_1|^2 &= 1 - |K_1|^2 = 1 - |K_2|^2 \end{aligned}$$

For a length  $\theta$  of a transmission line

$$\begin{vmatrix} I_1 \\ R_1 \end{vmatrix} = \begin{vmatrix} e^{j\theta} & 0 \\ 0 & e^{-j\theta} \end{vmatrix} \begin{vmatrix} R_2 \\ I_2 \end{vmatrix} \quad (15)$$

For a step change of characteristic impedance

$$\begin{vmatrix} I_1 \\ R_1 \end{vmatrix} = \frac{1}{T} \begin{vmatrix} 1 & K \\ K & 1 \end{vmatrix} \begin{vmatrix} R_2 \\ I_2 \end{vmatrix} \quad (16)$$

where

$$\begin{aligned} K &= \frac{Z_2 - Z_1}{Z_2 + Z_1} \\ T &= \frac{2\sqrt{Z_1 Z_2}}{Z_2 + Z_1} \end{aligned} \quad (17)$$

$Z_1$  being input characteristic impedance.

$Z_2$  being output characteristic impedance.

## References

- (1) "Very High-Frequency Techniques," by the Staff of the Radio Research Laboratory, Harvard University, page 685, McGraw Hill, New York, 1947.
- (2) H. B. Yin and T. U. Foley, "Filter using coaxial transmission line as elements," R.C.A. Review, Vol. XV, 1954, p. 62.
- (3) G. L. Ragan (Ed.), "Microwave Transmission Circuits," Radiation Lab. Series, Vol. 9, p. 551, McGraw Hill, New York, 1948.
- (4) A. E. Laemmel, "Scattering Matrix Formulations of Microwave Networks," Proc. Symposium on Modern Networks Synthesis, Polytechnic Institute of Brooklyn, New York, 1952, p. 259.

# THE USE OF A HORIZONTAL DIPOLE AS A DIRECTION FINDING AERIAL

BY G. MILLINGTON, M.A., B.Sc., M.I.E.E.

*In this paper the general problem of the use of a horizontal dipole as a direction finder is considered in relation to the type of wave radiated by the transmitter. The errors discussed are those due to field components which may exist under the ideal conditions assumed of a smooth homogeneous earth as distinct from site and instrumental errors. Part I refers especially to the use of an electric dipole direction finder at distances large compared with the terminal heights, while in Part II shorter distances and large angles of elevation are considered. In Part III the vertical frame regarded as a horizontal magnetic dipole is compared with the electric dipole and it is shown that it is subject to similar errors at the very high frequencies at which electric dipole is used.*

## PART I

### Introduction

FOR a transmitter which has an ideal horizontal dipole aerial, the electric field at points in the vertical plane through the centre of the dipole and perpendicular to its axis will be wholly horizontal and parallel to the axis of the dipole. It follows that a horizontal receiving dipole placed at the point will pick up no signal when it is turned towards the transmitter. This suggests the use of such a dipole as a simple form of direction finder for ultra-short waves where horizontal polarization is often used. The successful use of such a system depends upon the freedom from site errors and re-radiation from neighbouring objects, and upon the reception being effectively due to a ground wave with no appreciable reflections from the ionosphere or troposphere. Such a direction finder would be relatively sensitive compared with the usual differential type of rotating frame or spaced aerial system.

Apart, however, from the assumption that there is no polarization error due to the distortion of the wave in transmission, the accurate use of such a direction finder implies that the transmitting dipole is placed so that it is "broadside-on" to the receiver, and that it has no vertical component. If it is turned round so that it is "end-on" to the receiver, the horizontal electric field transverse to the direction of transmission reduces to zero, and an unwanted horizontal field in the direction of transmission increases from zero to a maximum. In the "end-on" position this longitudinal field is the only horizontal component of the electric field, and the horizontal receiving dipole would give a 90° error in the bearing. Compared with the maximum value of the wanted signal in the "broadside-on" position, this unwanted signal is very small, especially when the receiving dipole is raised above the ground, so that the errors it will introduce in the bearing will be small, except when observations are made very nearly in the "end-on" position, where the signal will in any case be small.

In practice the usefulness of the horizontal dipole as a direction finder is much more likely to be affected by a vertical component in the transmitting dipole which will produce a horizontal component of electric field along the direction of transmission independent of the azimuth. If, for instance, the transmitter is an aeroplane,

either by direct transmission from an aerial, or by re-radiation of an incident wave, such a vertical component of the transmitter regarded as an equivalent dipole is almost certain to be present, especially when the aeroplane banks and turns. The unwanted component of electric field due to this cause will often be large compared with that due to the horizontal dipole itself, especially near the end-on position.

It is the purpose of this article, therefore, to investigate the effect of this vertical component of the transmitting dipole on the use of a horizontal dipole as a direction finder. The horizontal component of electric field associated with this vertical component is due to the imperfect conduction of the earth, the consequent absorption of energy causing the electric vector in the wave to tilt forwards. This tilt obviously is reduced as the receiver is moved away from the ground, and we wish to determine the height to which it must be raised to ensure any desired performance as a direction finder.

### **General Analysis of the Horizontal Electric Field from a Transmitting Dipole**

We will suppose that the transmitting dipole makes an angle  $\theta$  with the horizontal, and that its horizontal projection makes an angle  $\phi$  with the "broadside-on" position. If the radiated power is  $P$ , the dipole is equivalent to a vertical dipole radiating  $P \sin^2\theta$ , a "broadside-on" dipole radiating  $P \cos^2\theta \cos^2\phi$ , and an "end-on" dipole radiating  $P \cos^2\theta \sin^2\phi$ . This last dipole we will neglect in comparison with the effects produced by the other two equivalent dipoles.

We shall make the following assumptions:—

- (1) The investigation is restricted to ultra-short waves for which the attenuation with distance is the same for vertically as for horizontally polarized waves.
- (2) The distance between the transmitter and receiver is large compared with the height of either above the ground.
- (3) The transmitter is far enough above the ground to remove the effect of earth losses in its immediate neighbourhood.
- (4) If the receiver is within the visual range of the transmitter, it is kept well below the height at which the first maximum of the interference pattern with raised transmitter and receiver occurs.
- (5) The receiver is sufficiently far from the transmitter to make the "numerical-distance" for a vertically polarized wave large.

These conditions will be satisfied in practice on ultra-short waves for many conditions in which direction finding measurements are likely to be made on a horizontal dipole. When they hold, the essential relationships between the various components of the electric field at the receiver are the same whether we are in the visual range and use the "flat-earth" type of analysis, or beyond the visual range where we use the complete diffraction analysis.

Let us suppose that when the receiver is on the ground, the vertical electric field due to the vertical component of the transmitting dipole is  $E_0^v$ . Then under our conditions, the wanted horizontal field on the ground due to the equivalent "broadside-on" dipole is  $E_0^h$  given by

$$E_0^h = \frac{\zeta_h}{\zeta_v} \cot \theta \cos \phi E_0^v$$

where account has been taken of the relative radiated powers of the two equivalent dipoles.  $\zeta_h$  is the earth constants function for horizontal polarization given by

$1/\sqrt{\epsilon-1-j60\sigma\lambda}$ , and  $\zeta_v$  is the corresponding function for vertical polarization given by  $(\epsilon-j60\sigma\lambda)/\sqrt{\epsilon-1-j60\sigma\lambda}$  in which  $\epsilon$  is the dielectric constant of the ground referred to air as unity, and  $\sigma$  is the conductivity in mhos per metre and  $\lambda$  is wavelength in metres.

When the receiver is raised above the ground to a height  $h$ , the initial form of the height-gain factor for the horizontally polarized wave is  $1 + j\frac{2\pi h}{\lambda\zeta_h}$ , so that the horizontal electric field is given by

$$E^h = \frac{\zeta_h}{\zeta_v} \left( 1 + j\frac{2\pi h}{\lambda\zeta_h} \right) \cot \theta \cos \varphi E_0^v$$

$$= \left( \zeta_h + j\frac{2\pi h}{\lambda} \right) \cot \theta \cos \varphi \frac{E_0^v}{\zeta_v}$$

Now over the range in which this form of the height-gain factor is valid, the unwanted horizontal component of the electric field in the direction of transmission due to the equivalent vertical dipole does not alter appreciably with the height, but retains its ground value, say  $E'$ , which is given by

$$E' = \frac{1}{\zeta_v} E_0^v$$

and gives a measure of the tilt of the electric vector on the ground for a vertically polarized wave due to earth losses. As the height increases, the tilt gets less, since the vertical field increases while the horizontal field remains practically unaltered.

At the height  $h$ , therefore, the ratio of the unwanted horizontal field  $E'$  to the wanted field  $E^h$  is given by

$$\frac{E'}{E^h} = \frac{\tan \theta \sec \varphi}{\zeta_h + j\frac{2\pi h}{\lambda}}$$

In this relation,  $\tan \theta$  represents the effect of tilting the transmitting dipole away from the horizontal by an angle  $\theta$ , and the factor  $\sec \varphi$  represents the result of turning the dipole away from the "broadside-on" position by an angle  $\varphi$ .

For the particular case when  $\varphi = 0$  and  $\theta = 45^\circ$ , we have

$$\frac{E'}{E^h} = \frac{1}{\zeta_h + j\frac{2\pi h}{\lambda}} \quad (\varphi = 0, \quad \theta = 45^\circ)$$

and on the ground

$$\frac{E'}{E^h} = \frac{1}{\zeta_h} \quad (\varphi = 0, \quad \theta = 45^\circ, \quad h = 0)$$

On ultra short waves,  $\zeta_h$  reaches its limiting value of  $1/\sqrt{\epsilon-1}$  where  $60\sigma\lambda \ll \epsilon$ , and for propagation over land, for which we take  $\epsilon = 5$ ,  $\zeta_h = 0.5$ , and is wholly real.

Thus on the ground  $E'/E^h = 2$ , and the unwanted signal is twice as strong as the wanted signal and in phase with it. The horizontal dipole used as a direction finder will give a zero minimum, but displaced by an angle  $\tan^{-1} 2 = 63.5^\circ$  from the true

direction of transmission. As the height is increased, the ratio  $E'/E^h$  becomes complex, the bearing being displaced and the minimum flattened. The term  $j\frac{2\pi h}{\lambda}$  rapidly becomes predominant over  $\zeta_h$  and their ratio, which is  $j\frac{4\pi h}{\lambda}$  for  $\zeta_h = 0.5$ , becomes  $j2\pi$  when  $h$  has increased to  $\frac{\lambda}{2}$ .

For propagation oversea,  $\zeta_h$  has a limiting value of about 0.1, so that the error in the bearing is initially greater on the ground than for overland propagation. But the term  $j\frac{2\pi h}{\lambda}$  becomes more rapidly predominant over  $\zeta_h$ , and their ratio is  $j2\pi$  when  $h$  is only  $\lambda/10$ , i.e. under all practical conditions. Thus in both cases we may say that when the receiver is more than half a wave-length above the ground

$$\frac{E'}{E^h} = -j\frac{\lambda}{2\pi h} \left( \varphi = 0, \quad \theta = 45^\circ \quad h > \frac{\lambda}{2} \right)$$

The resultant polarization in the horizontal plane is thus elliptical with the major axis in the wanted direction of  $E^h$  and the minor axis in the unwanted direction of  $E'$ . The horizontal dipole used as a direction finder should therefore give a correct bearing but with an imperfect minimum, and its usefulness depends upon the ability to set it accurately at the minimum when this is not a true zero but corresponds to a signal of the order of  $\frac{\lambda}{2\pi h}$  times the maximum signal. When for instance the wave-length used is 5 metres the aerial has to be raised to a height of 8 metres to reduce the ratio of the minimum to maximum signal to 1/10, and to a height of 80 metres to reduce it to 1/100. As we have seen, these figures are modified by the factor  $\tan \theta \sec \varphi$  in the general case.

### General Conclusions

The above analysis shows that on ultra short waves, provided the receiver is more than half a wave-length above the ground, the resultant horizontal field is not in general plane polarized at right angles to the direction of transmission, but elliptically polarized with its major axis along this transverse direction. The minor axis along the direction of transmission is  $\frac{\lambda}{2\pi h} \tan \theta \sec \varphi$  times the major axis. The behaviour of a horizontal receiving dipole as a direction finder improves as the height is increased or the wave-length is decreased, and the goodness of the bearing obtained depends upon the accuracy with which the dipole can be set to the position of minimum signal for a given minimum to maximum ratio. If the performance of the dipole as a function of this ratio is known, it is possible to estimate the height to which the dipole would have to be raised to obtain any desired performance.

It should be remembered that we have assumed an ideal set of conditions. Any distortion due to local site errors or re-radiation and reflection effects must be investigated experimentally to determine the probable error in bearing which may be so introduced. It should further be emphasized that we have assumed that, within the visual range, the angles of elevation of the transmitter and receiver are small. When this condition is waived, considerable errors may be obtained due to horizontal components of the field arising from the tilt of the electric vector produced

by the actual inclination of the wave front at the receiver. This effect can be dealt with separately by the method of geometrical optics. (See Part II.)

Finally, it is obvious that the successful use of a horizontal dipole as a direction finder depends upon the true behaviour of the dipole in picking up only horizontal fields. If the dipole were slightly tilted, or if there were any pick-up on the leads, the minima would be spoilt by a large residual signal due to vertical pick-up, since the radiation field in which the dipole is placed may contain large vertical components of electric field, as we have seen, which will be received by the dipole equally in all directions as it is rotated. It is therefore of great importance to adjust the dipole with extreme care to ensure that any such spurious vertical pick-up is too small to affect its performance as a direction finder.

## PART II

In Part I of this article the use of a horizontal dipole as a direction-finding aerial for ultra short waves was discussed, but it was assumed that the receiver was either below the line of sight of the transmitter or at a sufficiently great distance to make the angle of elevation of the transmitter at the receiver very small. It was shown that due to the tilt of the electric vector close to the ground, there is an unwanted horizontal component of the electric field along the direction of transmission when the transmitting aerial has a vertical component. As this tilt of the electric vector is due to the absorption of energy by the imperfectly conducting earth, the ratio of the unwanted component to the wanted transverse component of horizontal field becomes rapidly less as the height of the transmitter is raised, and the horizontal dipole used as a direction finder should then give a true bearing but with a flattened minimum. The ratio of the minimum to maximum signal is  $\frac{\lambda}{2\pi h} \tan \theta \sec \varphi$ , where  $h$  is the height of the receiver,  $\theta$  is the angle by which the transmitting dipole is tilted away from the horizontal, and  $\varphi$  is the azimuth angle through which it is turned from the "broadside-on" position.

It was pointed out, however, that when the angle of elevation gets large, this relation may no longer hold. Firstly, the height of the receiver may not be small, as was assumed, compared with the height at which the first maximum of the interference pattern with raised transmitter and receiver occurs, and secondly, the electric vector may be considerably tilted due to the actual inclination of the wave fronts arriving at the receiver, and produce an unwanted horizontal component of electric field independently of the imperfect conduction of the earth. Further, the "end-on" horizontal component of the transmitting dipole can for the same reason produce an unwanted horizontal component of electric field which is now of comparable importance, and which cannot be neglected as in the previous argument.

It is the purpose of this part of the article to investigate this aspect of the problem by the method of geometrical optics. For the angles of elevation with which we are now concerned, the curvature of the earth can be neglected, and on the ultra short waves we are considering, the effect of the surface wave can be neglected in comparison with the space wave. We can therefore treat the problem as the sum of a direct wave and a wave reflected from the earth for each of the components into which we resolve the transmitting dipole. We can, however, no longer treat the direct wave as the free space value in the equatorial plane of the transmitting dipole, but we must take into account the polar diagram whereby the electric field in a direction making an angle  $\theta$  with the axis of the dipole lies at right angles to this

direction in the plane containing the axis of the dipole, and has a magnitude  $\sin \theta$  times the corresponding equatorial field strength at the same distance. It will be assumed that the distance between the transmitter and the receiver is at least several wave-lengths, so that the inverse distance law for the free space field holds.

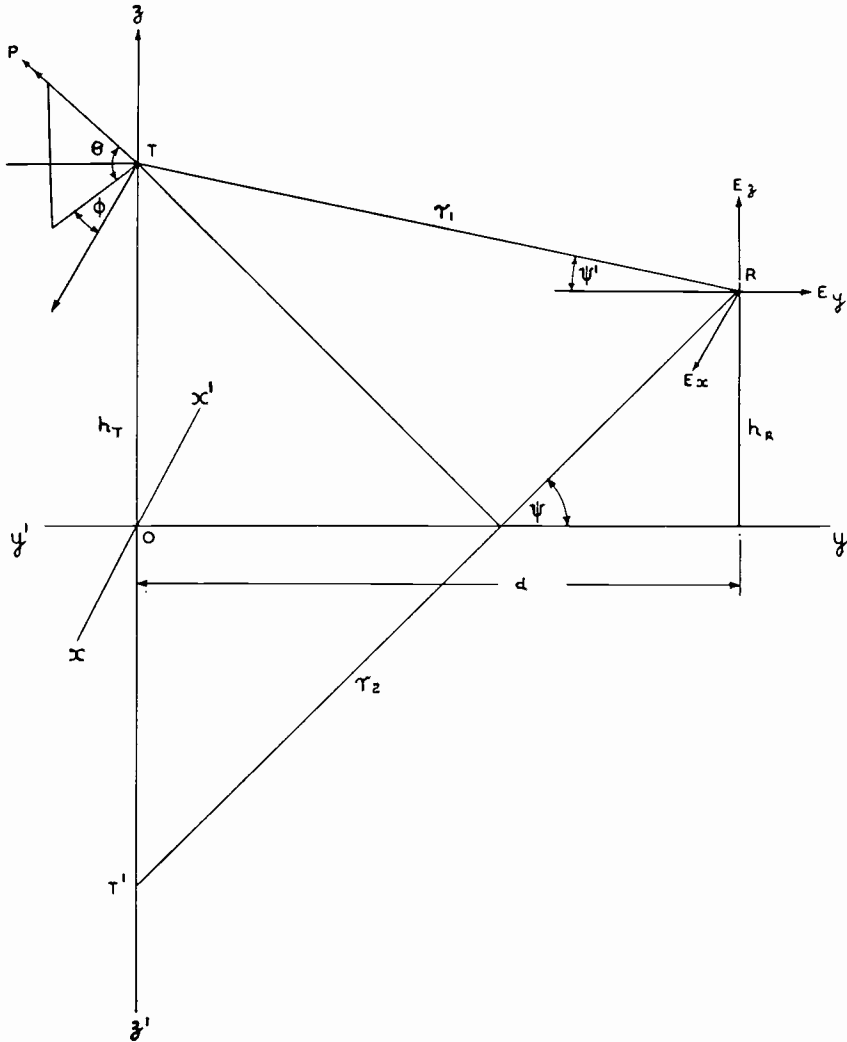


FIG. 1.  
*Geometry of the transmitting and receiving system for large angles of elevation.*

**General Analysis**

As before, we resolve our transmitting dipole into three equivalent dipoles, a vertical dipole with a moment proportional to  $\sin \theta$ , a "broadside-on" horizontal dipole with a moment proportional to  $\cos \theta \cos \phi$ , and an "end-on" horizontal dipole with a moment proportional to  $\cos \theta \sin \phi$ . In Fig. 1 the surface of the earth

is represented by the  $x\ 0\ y$  plane, and the transmitting dipole is placed at T, the point  $(0, 0, h_T)$ . The receiving dipole is placed at R, the point  $(0, d, h_R)$  in the  $y\ 0\ z$  plane. The axis of the transmitting dipole is along TP, so that the angles  $\theta$  and  $\phi$  are as shown. The "broadside-on" component is parallel to  $0\ x$ , and the "end-on" component is parallel to  $0\ y'$ , while the vertical component is along  $0\ z$ . At R, the electric field will have the components  $E_x, E_y, E_z$ , of which  $E_x$  is the wanted transverse horizontal field,  $E_y$  is the unwanted longitudinal horizontal field, and  $E_z$  is the vertical component which will only concern us in so far as the receiving dipole may not be a perfect horizontal dipole.

From the figure we see that if  $\Psi'$  is the angle of elevation of the transmitter at the receiver,

$$\tan \Psi' = \frac{h_T - h_R}{d} \quad (1)$$

and if  $\Psi$  is the angle of elevation of the receiver at the image T' of T in the ground,

$$\tan \Psi = \frac{h_T + h_R}{d} \quad (2)$$

The distance  $r_1$  between the transmitter and receiver is given by

$$r_1 = d \sec \Psi' \quad (3)$$

while the length of the reflected wave path is equal to the distance  $r_2$  between the image T' and the receiver, and is given by

$$r_2 = d \sec \Psi \quad (4)$$

Thus the path difference  $p$  between the direct and reflected wave paths is

$$p = r_2 - r_1 = d (\sec \Psi - \sec \Psi') \quad (5)$$

and the phase angle between the waves arriving at R is  $\delta$  where

$$\delta = \frac{2\pi p}{\lambda} = \frac{2\pi d}{\lambda} (\sec \Psi - \sec \Psi') \quad (6)$$

The reflection coefficient  $\rho_v$  for vertically polarized waves for the angle of elevation  $\Psi$  is

$$\rho_v = \frac{\zeta_v \sin \Psi - 1}{\zeta_v \sin \Psi + 1} \quad (7)$$

where

$$\zeta_v = \frac{\epsilon - j60\sigma\lambda}{\sqrt{\epsilon - \cos^2 \Psi - j60\sigma\lambda}} \quad (8)$$

and similarly for horizontally polarized waves

$$\rho_H = \frac{\zeta_H \sin \Psi - 1}{\zeta_H \sin \Psi + 1} \quad (9)$$

where

$$\zeta_H = \frac{1}{\sqrt{\epsilon - \cos^2 \Psi - j60\sigma\lambda}} \quad (10)$$

for an assumed time factor  $\exp(j\omega t)$ .

For ultra-short waves we can usually assume that the dielectric constant  $\epsilon \gg 60\sigma\lambda$ .

We then have

$$\zeta_v = \frac{\epsilon}{\sqrt{\epsilon - \cos^2 \Psi}} \quad (11)$$

and

$$\zeta_H = \frac{1}{\sqrt{\epsilon - \cos^2 \Psi}} \quad (12)$$

so that  $\zeta_v$  and  $\zeta_H$ , and hence  $\rho_v$  and  $\rho_H$  are both wholly real. If  $\epsilon \gg 1$ , we do not make any great error by writing  $\zeta_v = \sqrt{\epsilon}$  and  $\zeta_H = \frac{1}{\sqrt{\epsilon}}$ , independently of the value of  $\Psi$ , and in any particular case the error may only be comparable with the uncertainty in the value of  $\epsilon$ .

In order to find the required fields  $E_x$ ,  $E_y$ , and  $E_z$  at R, we determine the contributions due to each of the equivalent transmitting dipoles. In so doing, we have to adopt a convention with regard to the sense in which  $\theta$  and  $\phi$  are measured. As suggested in Fig. 1, we will measure  $\theta$  positive when TP is tilted upwards from the 0  $x$  direction, and  $\phi$  positive for a clockwise rotation from 0  $x$ . We need then only

to consider  $\theta$  and  $\phi$  over the range  $-\frac{\pi}{2}$  to  $\frac{\pi}{2}$  to give us all possible positions of the

transmitting dipole, remembering that a mere reversal of direction of the axis of the dipole is immaterial. It is convenient to express our fields in terms of  $E_0$ , the field that would be obtained at a distance  $d$  in the equatorial plane of the dipole in free space.

In terms of  $E_0$ , the total field of the direct wave from T to R for the equivalent vertical dipole will be  $E_0 \frac{d}{r_1} \sin \theta \cos \Psi'$ . The factor  $\sin \theta$  is due to the reduced moment of the vertical dipole, and the factor  $\cos \Psi'$  arises from the polar diagram of the dipole. By using (3), this field may be written  $E_0 \sin \theta \cos^2 \Psi'$ , and by resolving, it contributes a field  $E_0 \sin \theta \cos^3 \Psi'$  to  $E_z$ , and a field  $E_0 \sin \theta \sin \Psi' \cos^2 \Psi'$  to  $E_y$ . For the reflected wave the total field, allowing for the reflection coefficient and the path difference is given by  $E_0 \sin \theta \cos^2 \Psi' \rho_v e^{-j\delta}$ , giving contributions  $E_0 \sin \theta \cos^3 \Psi' \rho_v e^{-j\delta}$  and  $E_0 \sin \theta \sin \Psi' \cos^2 \Psi' \rho_v e^{-j\delta}$  to  $E_z$  and  $E_y$  respectively. If we consider the other equivalent dipoles in a similar manner; we can express our results as follows:—

(a) For the Equivalent Vertical Dipole:

$$\left. \begin{aligned} E_x &= 0 \\ E_y &= E_0 \sin \theta [\sin \Psi' \cos^2 \Psi' - \rho_v e^{-j\delta} \sin \Psi' \cos^2 \Psi'] \\ E_z &= E_0 \sin \theta [\cos^3 \Psi' + \rho_v e^{-j\delta} \cos^3 \Psi'] \end{aligned} \right\} \quad (13)$$

(b) For the equivalent "Broadside-on" Horizontal Dipole:

$$\left. \begin{aligned} E_x &= E_0 \cos \theta \cos \phi [\cos \Psi' + \rho_H e^{-j\delta} \cos \Psi'] \\ E_y &= 0 \\ E_z &= 0 \end{aligned} \right\} \quad (14)$$

(c) For the Equivalent "End-on" Horizontal Dipole:

$$\left. \begin{aligned} E_x &= 0 \\ E_y &= E_0 \cos \theta \sin \varphi [-\sin^2 \Psi' \cos \Psi' + \rho_v e^{-j\delta} \sin^2 \Psi' \cos \Psi] \\ E_z &= E_0 \cos \theta \sin \varphi [-\sin \Psi' \cos^2 \Psi' - \rho_v e^{-j\delta} \sin \Psi' \cos^2 \Psi] \end{aligned} \right\} \quad (15)$$

From (13), (14) and (15), the total fields  $E_x$ ,  $E_y$ , and  $E_z$  due to the actual transmitting dipole can be put in the form

$$\left. \begin{aligned} E_x &= E_0 A \cos \theta \cos \varphi \\ E_y &= E_0 [B \sin \theta + C \cos \theta \sin \varphi] \\ E_z &= E_0 [D \sin \theta + F \cos \theta \sin \varphi] \end{aligned} \right\} \quad (16)$$

where

$$\left. \begin{aligned} A &= \cos \Psi' + \rho_H e^{-j\delta} \cos \Psi' \\ B &= \sin \Psi' \cos^2 \Psi' - \rho_v e^{-j\delta} \sin \Psi' \cos^2 \Psi \\ C &= -\sin^2 \Psi' \cos \Psi' + \rho_v e^{-j\delta} \sin^2 \Psi' \cos \Psi \\ D &= \cos^3 \Psi' + \rho_v e^{-j\delta} \cos^3 \Psi \\ F &= -\sin \Psi' \cos^2 \Psi' - \rho_v e^{-j\delta} \sin \Psi' \cos^2 \Psi \end{aligned} \right\} \quad (17)$$

From the definitions of  $\Psi'$  and  $\Psi$  in (1) and (2), it will be seen that  $A$ ,  $C$  and  $D$  are symmetrical functions with respect to  $h_T$  and  $h_R$ , while  $F$  becomes equal to  $B$  when  $h_T$  and  $h_R$  are interchanged, as can be inferred by applying the reciprocal theorem to the various components of the field. It will be noted that we must regard  $\sin \Psi'$  as negative when  $h_T < h_R$ .

For a given wavelength, and for a given set of values of  $h_T$ ,  $h_R$ , and  $d$ ,  $A$ ,  $B$ , etc. in (17) are constant, independently of the values of  $\theta$  and  $\varphi$ , so that, having computed them, it is a fairly simple matter to study the change in the apparent bearing as the orientation of the transmitting dipole is changed. Further, in studying the effect of changing the wavelength,  $\lambda$  only enters the expressions for  $A$ ,  $B$ , etc. through the phase angle  $\delta$  given in (6), (and through the values of  $\rho_v$  and  $\rho_H$  if we cannot assume that  $\epsilon \gg 60\sigma\lambda$ ), so that it is not difficult to adjust the values of  $A$ ,  $B$ , etc. for a change of  $\lambda$  when  $h_T$ ,  $h_R$ , and  $d$  remain fixed.

It is convenient to express  $E_x$ ,  $E_y$ , and  $E_z$  in (4) in the form

$$\left. \begin{aligned} E_x &= E_0 R_x e^{j\gamma_x} \\ E_y &= E_0 R_y e^{j\gamma_y} \\ E_z &= E_0 R_z e^{j\gamma_z} \end{aligned} \right\} \quad (18)$$

The electric field in the horizontal plane will then be represented by the ellipse

$$\frac{E_y}{E_x} = \frac{R_y}{R_x} e^{j(\gamma_y - \gamma_x)}$$

If it should happen that  $\gamma_y - \gamma_x = 0$ , the field will be plane polarized, and the horizontal receiving dipole will pick up no signal when it is set at an angle  $\tan^{-1} \frac{R_y}{R_x}$

to the  $E_y$  direction, i.e. there will be a perfect minimum but the bearing will be displaced by an angle  $\tan^{-1} \frac{R_y}{R_x}$ . If  $\gamma_y - \gamma_x = \pm \frac{\pi}{2}$ , the axes of the polarization ellipse will lie along the  $E_x$  and  $E_y$  directions, and either a true bearing or a  $90^\circ$  error will be obtained, but with a flattened minimum, according as  $R_y$  is less or greater than  $R_x$ . In general  $\gamma_y - \gamma_x$  has some intermediate value, and for a given value of  $\gamma_y - \gamma_x$  the position and ratio of the axes of the ellipse will vary with the value of  $R_y/R_x$ . Their position relative to the  $E_x$  and  $E_y$  directions and their ratio can be read from some charts which have been given elsewhere,\* which are immediately applicable to the present problem.

It is not easy to see from the form of our expressions the way in which the errors in bearing obtained on the receiving dipole will vary with a change of any of the parameters  $\theta$ ,  $\phi$ ,  $h_T$ ,  $h_R$ ,  $d$ , and  $\lambda$ . A change in wave-length, for instance, may produce a large effect if we are in a region where the phase angle  $\delta$  is large and interferences can occur. It is probably best to work out one or two typical cases to show the nature of the errors that can be obtained. Before doing so, it may be pointed out, as in Part I, that it is very important to adjust the horizontal dipole so that it does not pick up any appreciable signal from the vertical field  $E_z$ , since we can see that this field is of the same order as the wanted field  $E_x$  in our present case.

### EXAMPLES

As a typical example we will take a receiving dipole at the top of a mast sixty metres high being used as a direction finder for an aeroplane flying at a height of 6,000 m. at a distance 20 km. away, i.e.,  $h_T = 6,000$  m,  $h_R = 60$  m. and  $d = 20$  km.

From (1) and (2) we find that  $\Psi' = 16^\circ 33'$  and  $\Psi = 16^\circ 51'$ , and from (17)

$$\left. \begin{aligned} A &= 0.959 + 0.957 \rho_H e^{-j\delta} \\ B &= 0.2615 - 0.266 \rho_V e^{-j\delta} \\ C &= -0.0777 + 0.0804 \rho_V e^{-j\delta} \\ D &= 0.881 + 0.877 \rho_V e^{-j\delta} \\ F &= -0.2615 - 0.266 \rho_V e^{-j\delta} \end{aligned} \right\} \quad (19)$$

For the path difference  $p$ , the factor  $\sec \Psi - \sec \Psi'$  in (5) is difficult to determine accurately when  $\Psi$  and  $\Psi'$  are nearly equal, and in our case where  $h_R \ll h_T$  and  $d$ ,  $p$  is given accurately by  $2h_T h_R / \sqrt{d^2 + h_T^2}$ , whence we have  $p = 34.45$  metres. Thus if we have a wave-length even as large as 10 m. the path difference will contain several whole wave-lengths, and a relatively small change in wave-length will suffice to alter the phase angle  $\delta$  by  $\pi$ .

If we take  $\lambda = 10$  m. we cannot assume that  $\epsilon \gg 60\sigma\lambda$  in fact for propagation oversea for which  $\epsilon = 80$  and  $\sigma = 4$ ,  $60\sigma\lambda \gg \epsilon$ .  $\zeta_V$  and  $\zeta_H$  are not wholly real, and for our value of  $\Psi$  we have by computation from (7), (8), (9) and (10),

#### *Propagation oversea*

$$\begin{aligned} \zeta_V &= 49.0 \quad \angle -44^\circ 3'. & \zeta_H &= 0.0204 \quad \angle 44^\circ 3' \\ \rho_V &= 0.904 \quad \angle -5^\circ 42'. & \rho_H &= -0.992 \quad \angle -0^\circ 24' \end{aligned}$$

---

\* T. L. Eckersley and G. Millington. Proc. Physical Society Vol. 51, pp. 110-128. 1939.  
See especially Figs. 5-9 with associated description on pp. 125-128.

For  $\rho_v$  the Brewster angle is of the order of  $1^\circ$ , and for our value of  $\Psi$ ,  $\rho_v$  is approaching the value 1, while  $\rho_H$  is nearly  $-1$

*Propagation overland*

$$\begin{aligned} \zeta_v &= 2.90 \angle -22^\circ 18'. & \zeta_H &= 0.371 \angle 27^\circ 54' \\ \rho_v &= -0.215 \angle 65^\circ 19' & \rho_H &= -0.828 \angle -5^\circ 47' \end{aligned}$$

For  $\rho_v$  we are near to the Brewster angle, and the phase angle of  $\rho_v$  is large. For  $\rho_H$  the phase angle is small, but appreciable compared with the phase angle for  $\rho_H$  oversea.

We can see from the expressions for  $A$ ,  $B$ , etc. that the errors in the bearing will depend intimately upon the phases of the terms  $\rho_v e^{-j\delta}$  and  $\rho_H e^{-j\delta}$ . Suppose for instance that we consider the value of the wanted field  $E_x$  in (16) which is proportional to  $A$ . In both cases above,  $|\rho_H|$  is comparable with unity, and the value of  $A$  when the phase angle of  $\rho_H e^{-j\delta}$  is  $\pm \pi$  will be small compared with the value when the phase angle is zero (omitting multiples of  $2\pi$ ). We should expect in general to get bigger errors in bearing when we happen to be at a trough than when we are at a crest in the interference pattern of the component  $E_x$ .

As mentioned above, we can pass from a crest to a trough by a relatively small change in wave-length in the case we are considering, but such a change in wave-length would modify slightly our computations for  $\rho_v$  and  $\rho_H$ . These computations also depend upon the value of  $\Psi$  used, but we can produce a change in the path difference without altering  $\Psi$ , by increasing or decreasing  $h_T$ ,  $h_R$  and  $d$  all by the same factor  $k$  by which we wish to modify  $p$  and hence  $\delta$ . If we consider the case of  $\lambda = 10$  m. for propagation oversea, we can make  $\rho_H e^{-j\delta} = 0.992$  and  $-0.992$  by making  $k = 1.015$  and  $1.16$  respectively. Even the latter change in the values of  $h_T$ ,  $h_R$  and  $d$  will not alter our problem materially as far as the order of the given heights and distance is concerned. The adjustment would of course be correspondingly smaller for a shorter wave-length.

By making these adjustments we get the following cases for propagation on  $\lambda = 10$  m. oversea:—

$$\begin{aligned} \text{(a) } \delta &= 179^\circ 36'. & \rho_v &= 0.904 \angle -5^\circ 42'. & \rho_v e^{-j\delta} &= -0.904 \angle -5^\circ 18' \\ & & \rho_H &= -0.992 \angle -0^\circ 24'. & \rho_H e^{-j\delta} &= 0.992 \\ \text{(b) } \delta &= -0^\circ 24'. & \rho_v e^{-j\delta} &= 0.904 \angle -5^\circ 18'. & \rho_H e^{-j\delta} &= -0.992. \end{aligned}$$

Case (a) will correspond to a crest and case (b) to a trough in the interference pattern of the wanted signal  $E_x$ . The contrast between the two cases will depend partly upon the effect of the adjustment we have made in  $\delta$  upon the unwanted signal  $E_y$ . If, for instance, the unwanted signal is at a trough when the wanted signal is also at a trough, and similarly they are at a crest together, the contrast will be less than when one is at a trough while the other is at a crest and vice-versa.

From our expressions in (19) we have for the values of  $\rho_v e^{-j\delta}$  and  $\rho_H e^{-j\delta}$  above:—

Case (a) $A = 1.908$	Case (b) $A = 0.010$
$B = 0.501 - j 0.0222$	$B = 0.022 + j 0.0222$
$C = -0.1500 + j 0.00670$	$C = -0.0054 - j 0.00670$
$D = 0.092 + j 0.0732$	$D = 1.670 - j 0.0732$
$F = -0.022 - j 0.0222$	$F = -0.501 + j 0.0222$

Now from (16) we have

$$\frac{E_y}{E_x} = \frac{B}{A} \tan \theta \sec \varphi + \frac{C}{A} \tan \varphi$$

so that we have

Case (a)

$$\frac{E_y}{E_x} = [0.262 - j 0.0116] \tan \theta \sec \varphi + [-0.0785 + j 0.00351] \sec \varphi$$

Case (b)

$$\frac{E_y}{E_x} = [2.2 + j 2.22] \tan \theta \sec \varphi + [-0.54 - j 0.67] \tan \varphi$$

It is obvious that in general the error produced in the bearing for a given pair of values of  $\theta$  and  $\varphi$  will be considerably greater in case (b) than in case (a).

Without giving the details of the computations, we can present the results graphically as in Figs. 2 and 3, where the error in the bearing, say  $\chi$ , is shown as a function of  $\theta$  for a set of values of  $\varphi$ . These curves should really be supplemented by a set of curves showing the sharpness of the minimum obtained, as measured by the ratio of the axes of the polarization ellipse, with some indication of the variation of the general level of the signals received. The curves are shown for both positive and negative values of  $\theta$  and for positive values of  $\varphi$ . For negative values of  $\varphi$  we obtain with positive or negative values of  $\theta$  the same error, but with sign reversed, as we do with  $\varphi$  positive and  $\theta$  negative or positive, since the reversal of both  $\theta$  and  $\varphi$  changes the position of the transmitting dipole to that of its mirror image in the vertical plane of transmission, and the apparent bearing is accordingly merely reversed in sign.

In Fig. 2 for case (a), the marked difference in the curves for a given value of  $\varphi$ , according as  $\theta$  is positive or negative, is due to the fact that the unwanted signal  $E_y$  is made up of two components, one due to the vertical and the other to the end-on component of the transmitting dipole, which tend to oppose for  $\varphi$  positive when  $\theta$  is positive and to add when  $\theta$  is negative. The phase angle of  $E_y/E_x$  is everywhere small, so that in this case the position of the apparent bearing should be well defined. When  $\theta$  is positive, the error is comparatively small for values of  $\varphi$  up to  $80^\circ$  so long as  $\theta$  is less than  $20^\circ$ , but when  $\theta$  is negative, we see that we can get a  $10^\circ$  error when  $\theta$  is only  $20^\circ$  and  $\varphi$  about  $30^\circ$ , or when  $\theta = 30^\circ$  and  $\varphi$  nearly zero.

In the less favourable case (b) shown in Fig. 3, we can get an error of about  $25^\circ$  when  $\theta$  is  $10^\circ$  and  $\varphi$  is zero, while for  $\theta = -10^\circ$  and  $\varphi = 30^\circ$  the error is  $50^\circ$ . The curves for  $\varphi$  greater than  $30^\circ$  are not shown, as it is obvious that in general the errors will be extreme even for small values of  $\theta$ . In this case the unwanted field  $E_y$  is in general about  $45^\circ$  out of phase with the wanted field, and the definition of the apparent bearing will be poorest, corresponding to a minimum to maximum ratio of 0.4, when the error in bearing is about  $45^\circ$ .

It must be remembered that cases (a) and (b) represent neither the most nor the least favourable cases, which would be given when the wanted signal was at a crest and the unwanted signal was at a trough and vice versa, whereas in case (a) they are nearly at a crest together, and in case (b) at a trough together\*. But they are amply

---

\*For propagation overland under similar conditions, the troughs of the unwanted signal are much less marked as  $|\rho_v|$  is only of the order of 0.2. We would tend therefore to get conditions rather more favourable than case (a) when the wanted signal is at a crest, and even less favourable than case (b) when it is at a trough.

The Use of a Horizontal Dipole as a Direction Finding Aerial

sufficient to show that under practical conditions in which a horizontal dipole might be used for locating aircraft flying at a great height, the errors in bearing obtained may be extreme. We may also again stress the fact that large errors would also be produced if the horizontal dipole were not perfect as regards picking up no signal

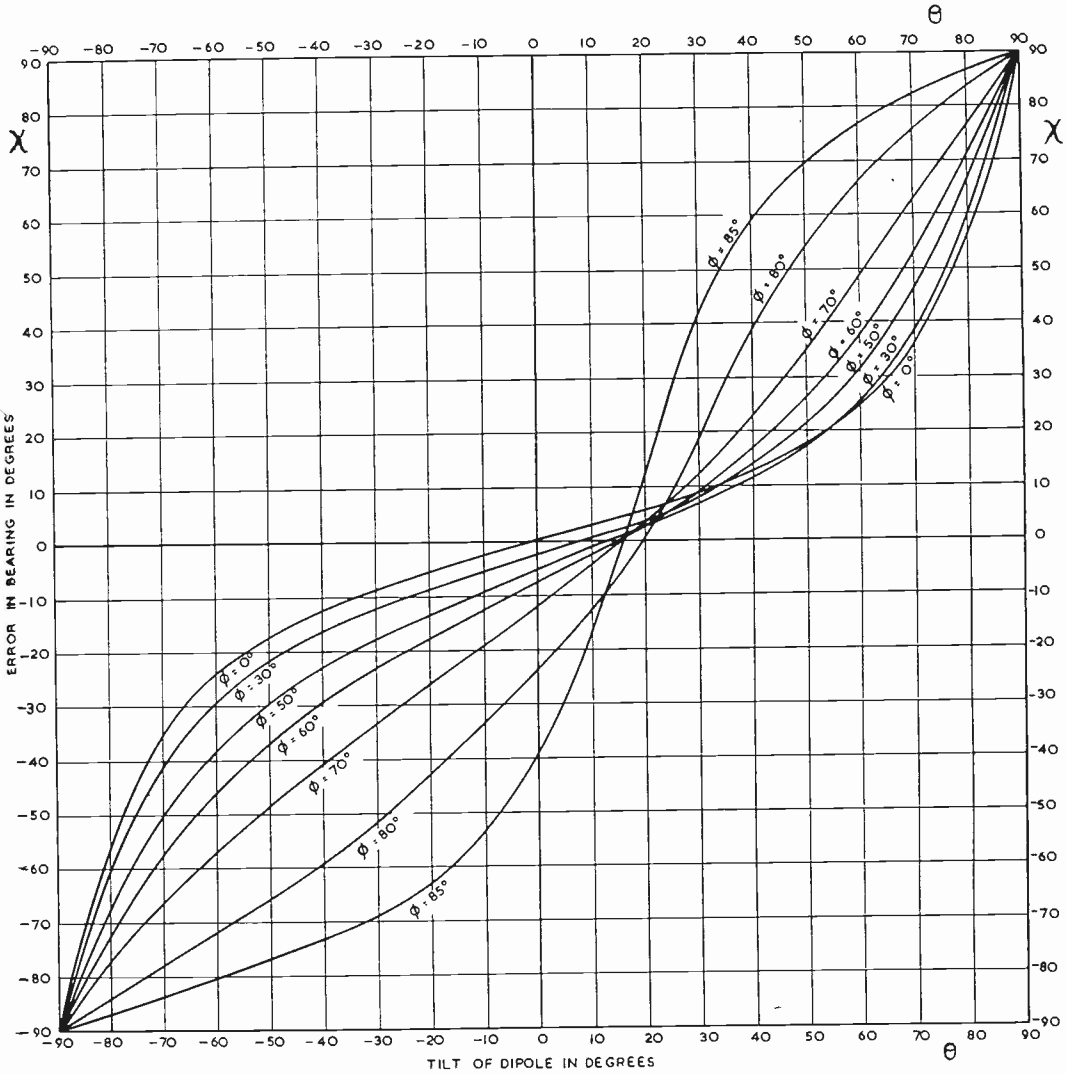


FIG. 2.

Error in Bearings on a Horizontal Receiving Dipole.

$b_T = 6000M, b_R = 60M, d = 20kM$  wanted signal at a crest.

$\theta =$  Tilt of transmitting dipole at an azimuth  $\phi$  to the broadside position.

from the vertical component of the electric field. By using the values of  $D$  and  $F$  in (19), we can see that the unwanted vertical component  $E_z$  is of the same type and order as the unwanted field  $E_y$ .

**Conclusion**

The examples given above are typical in showing that the bearings obtained on a horizontal electric dipole when the angles of elevation are at all large may be extreme, and that they vary rapidly as the various parameters are altered. As in

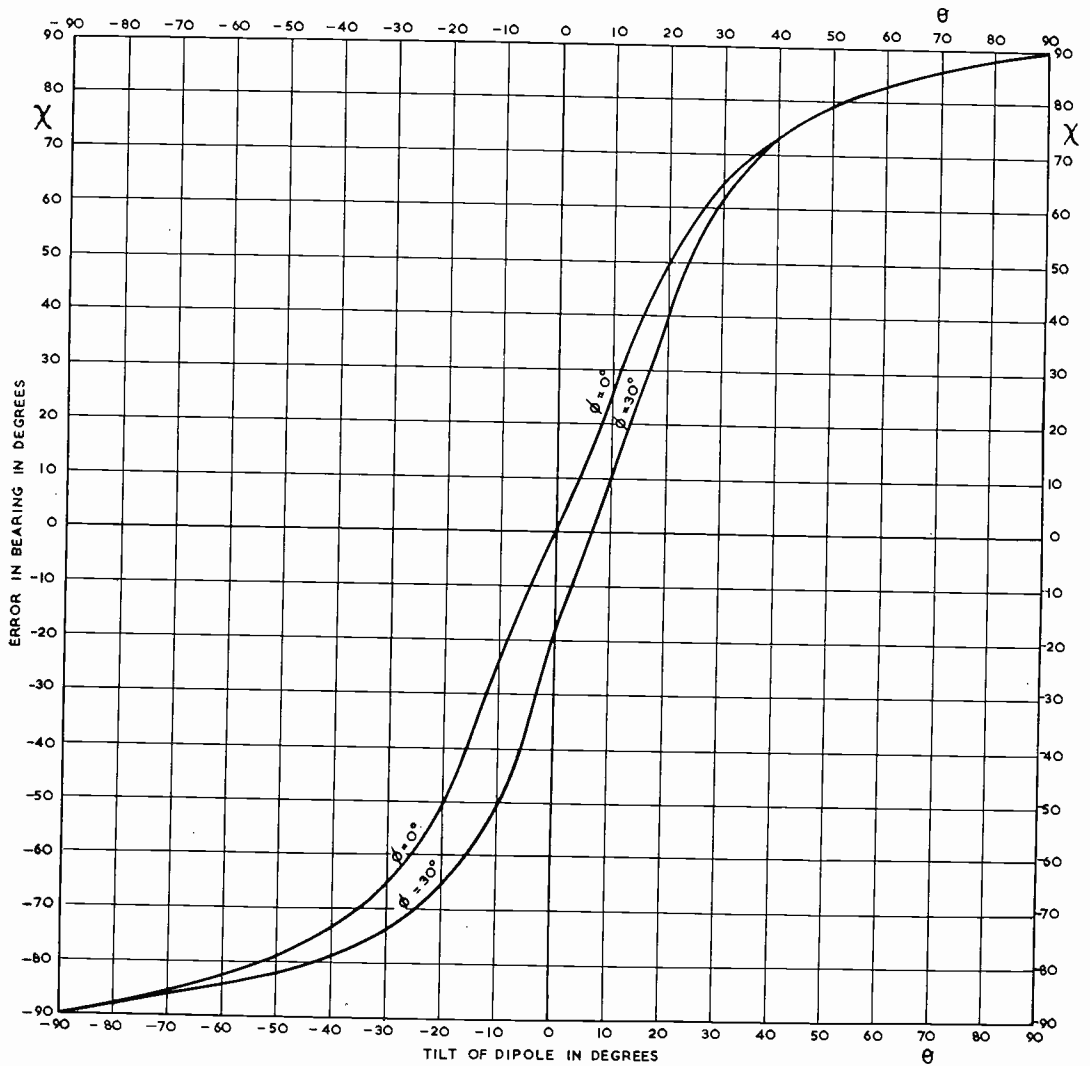


FIG. 3.

*Error in Bearings on a Horizontal Receiving Dipole.*

$\lambda = 10M, h_T = 600M, h_R = 60M, d = 20kM$  wanted signal at a trough.  $\theta$  tilt of transmitting dipole at an azimuth  $\phi$  to the broadside position.

practice, especially with an aeroplane as a transmitter, we have no precise knowledge of the values of these parameters at any given moment, we cannot tell whether any observed bearing is subject to only a small or to a very large error. The curves in Figs. 2 and 3 are intended not to show what precise error may be allotted to any

observed bearing obtained in practice, but to indicate the general order of the errors that will occur under any given conditions. They have been obtained by idealizing the transmission conditions, and in practice they will be modified in detail by various factors, such as a more complex aerial system than that assumed in the transmitting dipole, and distortion effects due to ground irregularities and atmospheric refraction.

We conclude, therefore, that a horizontal electric dipole cannot be used as a direction finder under such conditions as we have been considering. We have already discussed, in Part I, its limited use as a direction finder when the angles of elevation are very small or the receiver is below the line of sight of the transmitter. The analysis given here will provide a guide in fixing the probable accuracy of such a direction finder when the angles of elevation begin to get appreciable.

### PART III

In the third part of this article, we shall discuss the use of a vertical frame and of a horizontal dipole as direction finders with special application to ultra short waves.

It is well known that on medium and long waves a horizontally polarized wave transmitted over the surface of the earth is very rapidly attenuated with increasing distance compared with a vertically polarized wave, the contrast increasing as the wave length is increased. As a result of this differential attenuation, a wave which leaves the transmitter with a mixed polarization becomes predominantly vertically polarized at comparatively short distances, and it is upon this fact that the success of the simple vertical frame as a direction finding aerial depends, when it can be assumed that there are no polarization errors due to waves reflected from the ionosphere, and the transmission is solely by the ground wave.

When, however, the wave length is decreased, a limit is reached at which the attenuation with distance for the two types of polarization becomes effectively the same, and any polarization error present at a short distance may persist, however great the distance is made. The frame aerial can no longer be used as an accurate direction finder unless the transmitted wave leaves the aerial as a vertically polarized wave. If, for instance, the transmitting aerial has a horizontal top, or is a trailing wire or one that sags in a catenary, the transmitted wave may have a large horizontally polarized component which will produce a polarization error on the frame direction finder.

With the advances that have been made in high frequency technique, it is now possible to build a frame direction finder with a very good instrumental performance, and it is therefore a matter of considerable importance to study the problem of ground wave transmission over an ideal homogeneous spherical earth, to see how the type of wave transmitted affects the accuracy of bearings taken on such a frame. Such an investigation will form a most useful basis for predicting the probable performance of the frame under any actual conditions, though the errors which may be introduced by local site errors and ground irregularities must necessarily form the subject of a practical research to determine whether they will affect the results of a frame direction finder working under otherwise ideal conditions.

The practical equivalence of horizontal and vertical polarization on ultra short waves as far as attenuation with distance is concerned, has led to the use of horizontal transmitting dipoles on these wavelengths, and analogous to the use of the vertical frame for a vertically polarized wave, a horizontal dipole rotating about a vertical axis can be used as a direction finder when the axis of the transmitting dipole is at right angles to the vertical plane containing the transmitting and receiving points. In the same way, polarization errors will occur if the transmitting aerial

does not satisfy this condition. The behaviour of the horizontal dipole as a direction finder has already been discussed in Parts I and II of this article and it is our purpose here to show that the behaviour of the vertical frame is closely analogous to that of the horizontal dipole, and hence to deduce that the general results already obtained for the horizontal dipole apply also to the vertical frame.

By the principle of reciprocity the simple frame aerial and the electric dipole, which as we have shown can both be used for direction finding purposes, can both be used as directional transmitters, and what we wish to emphasize here is the analogy between the two aerials both in their transmitting and in their receiving properties. The behaviour of the electrical dipole is quite obvious. It is an aerial radiator or receiver which, in the simplest case, is a single rod, and all that we need to know about it as a receiver is its direction in space. As a transmitter its moment must be prescribed, and for a given current and frequency this moment may be specified in terms of the length of the dipole.

We have a similar definition in the case of the frame, or what we may call the magnetic dipole. In this, all we require to know is the direction in which the frame is oriented and the moment specified by  $\frac{2\pi A}{\lambda}$  where  $A$  is the area of the frame. In the ideal case, which when summed up produces any actual case, the vector perpendicular to the area and through its centre is sufficient to specify it exactly, and this way of specification emphasizes the analogy between the electric and magnetic dipoles, since each is specified uniquely by a scalar moment and a vector which gives the direction. It is only in the case of the electric dipole that this vector has a physical counterpart in the rod aerial itself, but the analogy shows that the magnetic dipole will be affected by the magnetic field of a received wave in the same way as the electric dipole is affected by the electric field.

### **Definitions and General Considerations**

We will define the horizontal direction at the receiver in the vertical plane containing the transmitting and receiving points as the direction of true bearing, and the components of the electric and magnetic fields in this direction as the longitudinal components which we will write as  $E_L$  and  $H_L$  respectively. The horizontal components at right angles to this direction we will call the transverse components  $E_T$  and  $H_T$ . The remaining components  $E_V$  and  $H_V$  are vertical. Thus the  $T$ ,  $L$ , and  $V$  components form a rectangular system which applies both to a flat earth and a curved earth.

When the horizontal electric or magnetic dipole is turned so that it lies along the direction of true bearing, it will be referred to as being in the longitudinal position with respect to the transmitter, and when it is at right angles to this direction it will be said to be in the transverse position. If we think of the magnetic dipole as a vertical frame, the longitudinal position can be regarded as the broadside position of the frame, and the transverse position as the edge-on position of the frame.

At the transmitter we can similarly define a set of rectangular axes consisting of longitudinal and transverse horizontal axes and a vertical axis. If the transmitter is an open aerial, it can be replaced for purposes of analysis by an electric dipole which may have any given orientation in space, but it can be resolved into a longitudinal, a transverse, and a vertical dipole in the  $T$ ,  $L$ , and  $V$  directions respectively. We are not so likely to have to consider a closed frame transmitting aerial, but it can be treated most simply as a magnetic dipole and resolved in the same way, and it will be formally included to complete the analogy.

*The Use of a Horizontal Dipole as a Direction Finding Aerial*

The electric dipole will function as a perfect direction finder if it is placed in an electric field in which there is a component  $E_T$  but no component  $E_L$ , it being unaffected by any component  $E_V$  that may be present. It then gives zero pick-up when it is set in the longitudinal position along the direction of true bearing. Alternatively, if there is an  $E_L$  but no  $E_T$  component, it will give a  $90^\circ$  error, but could theoretically be used as a direction finder by allowing for the rotation through  $90^\circ$ . In practice, of course, the  $E_L$  component is usually small under conditions in which  $E_T$  is zero. The horizontal magnetic dipole functions as a direction finder in a similar way with respect to the magnetic field, and will give a correct bearing in the longitudinal position (i.e. with the frame in the broadside position) when there is an  $H_T$  but no  $H_L$  component.

In the general case in which the electric (or magnetic) field has both  $T$  and  $L$  components, the field in the horizontal plane will be elliptically polarized, and the dipole will give a minimum when it is set along the minor axis of the ellipse. The bearing will be in general displaced, and depending on the ratio of the axes of the ellipse, the minimum will be flattened, except when the ellipse happens to degenerate into a straight line. Our problem can therefore be attacked by considering what the  $T$  and  $L$  components of  $E$  and  $H$  are for each of the resolved  $T$ ,  $L$  and  $V$  electric and magnetic dipoles constituting the transmitter. For this purpose it is useful to construct a table showing which of the components  $E_T$ ,  $E_L$ ,  $E_V$  and  $H_T$ ,  $H_L$ ,  $H_V$  can be present in the electromagnetic fields due to the various possible component dipoles of the transmitter.

TABLE OF COMPONENTS OF THE ELECTROMAGNETIC FIELD AT THE RECEIVER

Transmitting Dipole	Polarization	E <sub>T</sub>	E <sub>L</sub>	E <sub>V</sub>	H <sub>T</sub>	H <sub>L</sub>	H <sub>V</sub>
Electric Transverse ...	VMD	×				×	×
Electric Longitudinal ...	VED		×	×	×		
Electric Vertical ...	VED		×	×	×		
Magnetic Transverse ...	VED		×	×	×		
Magnetic Longitudinal ...	VMD	×				×	×
Magnetic Vertical ...	VMD	×				×	×

In this table a gap indicates that the component cannot be present, while a cross indicates that the component is in general present, though it may be of zero intensity in certain particular cases. The table gives no indication of the relative strengths of the various components for a given type of transmitting dipole. At first sight we might not expect to get a longitudinal field from a longitudinal dipole, but it must be remembered that we are not measuring our longitudinal field on the axis of the dipole in free space. The transmitting and receiving aerials are not necessarily at the same height above the ground, and even if they were, the presence of the earth would modify the field at the receiving point and produce in general a longitudinal component of the field, even though it might only be of relatively small amplitude in many cases. For each of the transmitting dipoles all the components of the electric and magnetic fields are of one characteristic type of polarization, either of the VED or the VMD types, and this is indicated in the column headed "polarization".\*

\*By VED and VMD are meant the characteristic polarizations associated with a vertical electric dipole and a vertical magnetic dipole respectively.

This information is useful when we want to see at a glance which components of the field will survive when the wave-length is increased and differential attenuation occurs.

Suppose, for instance, that we wish to consider the operation of a horizontal electric dipole in conjunction with an electric dipole transmitter. As mentioned above, it will give a correct bearing when the transmitting dipole is transverse, since there is then an  $E_T$  but no  $E_L$  component. But if the transmitting dipole also contains a longitudinal or a vertical component, there will be a component  $E_L$  introduced, and an error will consequently result. Moreover, while  $E_T$  is of VMD type,  $E_L$  is VED, and we see that such errors will be increasingly detrimental as the wave-length is increased.

If we use a horizontal magnetic dipole, it will give a correct bearing both for the longitudinal and vertical components of the electric dipole transmitter, while the error is introduced by the transverse component. In this case the error gets less detrimental as the wave-length is increased, and we notice that the transmitting dipole can be moved out of the vertical position without introducing any error, provided that it is kept in the vertical plane containing the transmitting and receiving points. Analogously, the magnetic transmitting dipole only gives an error with the horizontal electric dipole if it has a transverse component, while with the horizontal magnetic dipole it will produce an error if it has any longitudinal or vertical component. Here again an increase of wave-length differentiates in favour of the magnetic dipole or frame direction finder.

In order to determine the magnitude of the error to be expected in any given conditions, we must determine the values of the components of  $E$  and  $H$  by applying the known results of propagation theory. In so doing we will restrict ourselves to ultra short waves, as was done in discussing the horizontal electric dipole, for which the attenuation with distance is the same for both VED and VMD polarized waves. It was shown that two distinct cases arise, firstly when the distance is great enough to make the angles of elevation of the transmitter and its image very small at the receiver, as was assumed in Part I of the paper, and secondly when the angles of elevation are no longer small, as was considered in Part II. We shall briefly discuss these two cases in turn to show the analogy which we are considering here.

### **Analysis of the Problem for Small Angles of Elevation**

This case includes not only distances near to the edge of the visual range, but all those beyond it in the diffraction range, since the results we are to use are the same whether we use the flat earth theory for small angles of elevation or the complete diffraction analysis for a curved earth.

Let us suppose that we have two electric dipoles, a transverse one, and a vertical one, both on the ground and radiating equal powers. At a distance sufficiently great to make the angles of elevation very small, and for all points beyond in the diffraction region, there is a simple relation between the transverse electric field on the ground due to the transverse dipole, and the vertical electric field on the ground due to the vertical dipole, which is independent of the distance, as the attenuation with distance is the same for both types of polarization. If these fields are respectively  $E_T$  and  $E_V$ , this relation is

$$\frac{E_T}{E_V} = \frac{\zeta_H^2}{\zeta_V^2}, \quad (h_T = h_R = 0) \quad (1)$$

where  $\zeta_H$  and  $\zeta_V$  are the earth constant functions already defined in Part I. This

relation is independent of the number of terms of the diffraction formula which may have to be used. As  $\zeta_H$  is less than  $\zeta_V$  even at the dielectric limit, the ground value of  $E_T$  is always less than the ground value of  $E_V$ , and as with increasing wave-length  $\zeta_V$  increases while  $\zeta_H$  decreases (the relation  $\zeta_V \zeta_H = 1$  becoming rapidly true), the vertical field on the ground gets relatively strong compared with the transverse field, quite apart from any considerations of differential attenuation with distance.

If now both the transmitting aerials are raised to a height  $h_T$  above the ground, the initial height gain factors are  $1 + j \frac{2\pi h_T}{\lambda \zeta_H}$  and  $1 + j \frac{2\pi h_T}{\lambda \zeta_V}$  respectively. Thus we have

$$\frac{E_T}{E_V} = \frac{1 + j \frac{2\pi h_T}{\lambda \zeta_H}}{1 + j \frac{2\pi h_T}{\lambda \zeta_V}} \cdot \frac{\zeta_H^2}{\zeta_V^2} \quad (h_R = 0, h_T \text{ small}) \quad (2)$$

These forms of the height gain factor are still valid at the height where  $\frac{2\pi h_T}{\lambda \zeta_V} \gg 1$  (and, *a fortiori*,  $\frac{2\pi h_T}{\lambda \zeta_H} \gg 1$ , since  $\zeta_V > \zeta_H$ ) so that we have

$$\frac{E_T}{E_V} = \frac{\zeta_H}{\zeta_V} \left( h_R = 0, h_T \gg \frac{\lambda \zeta_V}{2\pi} \right) \quad (3)$$

Even when the initial form of the height-gain factors no longer holds, the ratio of the two factors remains  $\zeta_V/\zeta_H$  and the relation (3) is still true.

Now the vertical dipole produces a longitudinal field  $E_L$  which only alters slowly with the height of the receiver, so that for small heights it can be assumed to be independent of the height. It is simply related to the value of  $E_V$  on the ground ( $h_T$  not necessarily being zero), being given by

$$E_L = \frac{1}{\zeta_V} (E_V)_{h_R=0} \quad (\text{for } h_R \text{ small}) \quad (4)$$

But when the receiver is raised to a small height  $h_R$ , the height-gain factor is  $1 + j \frac{2\pi h_R}{\lambda \zeta_H}$

so that

$$E_T = \left( 1 + j \frac{2\pi h_R}{\lambda \zeta_H} \right) (E_T)_{h_R=0} \quad (\text{for } h_R \text{ small}) \quad (5)$$

thus from (4) and (5)

$$\frac{E_L}{E_T} = \frac{1}{\zeta_V \left( 1 + j \frac{2\pi h_R}{\lambda \zeta_H} \right)} \left( \frac{E_V}{E_T} \right)_{h_R=0} \quad (\text{for } h_R \text{ small}) \quad (6)$$

and from (3) we then have

$$\frac{E_L}{E_T} = \frac{1}{\zeta_V \left( 1 + j \frac{2\pi h_R}{\lambda \zeta_H} \right)} \cdot \frac{\zeta_V}{\zeta_H}$$

$$= \frac{1}{\zeta_H + j \frac{2\pi h_R}{\lambda}} \left( \text{for } h_R \text{ small, } h_T \gg \frac{\lambda \zeta_V}{2\pi} \right) \quad (7)$$

This ratio represents the horizontal polarization ellipse obtained at fairly small heights when the transmitter is raised well off the ground and consists of an electric dipole having equal transverse and vertical components. Under these conditions any longitudinal component of the transmitter would only produce a secondary effect to the value of  $E_L$ . If the transmitting dipole is tilted at an angle  $\theta$  from the horizontal and in an azimuth  $\varphi$  to the transverse position, the ratio of  $E_L/E_T$  in (7) becomes

$$\frac{E_L}{E_T} = \frac{\tan \theta \sec \varphi}{\zeta_H + j \frac{2\pi h_R}{\lambda}} \left( \text{for } h_R \text{ small, } h_T \gg \frac{\lambda \zeta_V}{2\pi} \right) \quad (8)$$

which is the relation already given in Part I where its significance was discussed.

From the analogy we are considering, we can derive a similar relation for  $H_L/H_T$ , expressing the behaviour of the magnetic dipole as a direction finder.

If we again have two equal transverse and vertical electric dipoles, the relation analogous to (1) is

$$\frac{H_V}{H_T} = \frac{\zeta_H^2}{\zeta_V^2} \quad (h_T = h_R = 0) \quad (9)$$

where  $H_V$  is due to the transverse dipole, and  $H_T$  due to the vertical dipole.

When both aerials are raised to the height  $h_T$ , the initial height gains are  $1 + j \frac{2\pi h_T}{\lambda \zeta_H}$  and  $1 + j \frac{2\pi h_T}{\lambda \zeta_V}$  as before, so that analogous to (2), we have

$$\frac{H_V}{H_T} = \frac{1 + j \frac{2\pi h_T}{\lambda \zeta_H}}{1 + j \frac{2\pi h_T}{\lambda \zeta_V}} \cdot \frac{\zeta_H^2}{\zeta_V^2} \quad (h_R = 0, h_T \text{ small}) \quad (10)$$

and similarly for heights for which  $h_T \gg \frac{\lambda \zeta_V}{2\pi}$ ,

$$\frac{H_V}{H_T} = \frac{\zeta_H}{\zeta_V} \left( h_R = 0, h_T \gg \frac{\lambda \zeta_V}{2\pi} \right) \quad (11)$$

The component  $H_L$  is now due to the transverse dipole. Analogously to  $E_L$ , it varies slowly with the height of the receiver and

$$H_L = \frac{1}{\zeta_H} (H_V)_{h_R=0} \quad (\text{for } h_R \text{ small}) \quad (12)$$

When the receiver is raised to a height  $h_R$ , the initial height gain factor for  $h_T$  is  $1 + j \frac{2\pi h_R}{\lambda \zeta_V}$ , and thus

$$H_T = \left(1 + j \frac{2\pi h_R}{\lambda \zeta_V}\right) (H_T)_{h_R=0} \quad (\text{for } h_R \text{ small}) \quad (13)$$

Thus for  $h_R$  small, we have from (12) and (13)

$$\frac{H_L}{H_T} = \frac{1}{\zeta_H \left(1 + j \frac{2\pi h_R}{\lambda \zeta_V}\right)} \left(\frac{H_V}{H_T}\right)_{h_R=0} \quad (\text{for } h_R \text{ small}) \quad (14)$$

and from (11) we then have

$$\begin{aligned} \frac{H_L}{H_T} &= \frac{1}{\zeta_H \left(1 + j \frac{2\pi h_R}{\lambda \zeta_V}\right)} \frac{\zeta_H}{\zeta_V} \\ &= \frac{1}{\zeta_V + j \frac{2\pi h_R}{\lambda}} \left(h_R \text{ small, } h_T > > \frac{\lambda \zeta_V}{2\pi}\right) \end{aligned} \quad (15)$$

If we have a transmitting dipole which is not vertical, but tilted towards the horizontal by an angle  $\theta$  at an azimuth  $\varphi$  to the transverse position, then (15) becomes

$$\frac{H_L}{H_T} = \frac{\tan \theta \cos \varphi}{\zeta_V + j \frac{2\pi h_R}{\lambda}} \left(h_R \text{ small, } h_T > > \frac{\lambda \zeta_V}{2\pi}\right) \quad (16)$$

As far as the denominator in (16) is concerned, in general the behaviour of  $\frac{H_L}{H_T}$  is similar to that of  $\frac{E_L}{E_T}$ . When  $h_R = 0$ , we have the factor  $\frac{1}{\zeta_V}$  instead of  $\frac{1}{\zeta_H}$  and the ratio of longitudinal to transverse field is less for the magnetic field than for the electric field, and the magnetic dipole is less subject to error on the ground than the electric dipole. As  $h_R$  is increased, the denominator of  $H_L/H_T$  remains greater than that of  $E_L/E_T$ , but when  $h_R > > \frac{\lambda \zeta_V}{2\pi}$ , they are in effect the same, and  $\frac{H_L}{H_T} = \frac{-j\lambda}{2\pi h_R}$ , apart from the factor  $\tan \theta \cos \varphi$ . The law of change with height becomes the same as for  $E_L/E_T$ , and the general remarks made about the electric dipole in Part I hold as well for the magnetic dipole.

In comparing the factors  $\tan \theta \sec \varphi$  and  $\tan \theta \cos \varphi$  in (8) and (16), we must remember that the angle of tilt  $\theta$  is measured from the horizontal in (8), and from the vertical in (16), since in the ideal case the electric dipole works in conjunction with a transverse transmitting dipole, and the magnetic dipole with a vertical transmitting dipole. The difference in the factors  $\sec \varphi$  and  $\cos \varphi$  arises from the fact that with the electric dipole, the effect of increasing  $\varphi$  is to weaken the wanted component  $E_T$ , while with the magnetic dipole it weakens the unwanted component  $H_L$ . We see that when  $\varphi = 90^\circ$ , there is no error with the magnetic dipole, as mentioned above. The indeterminate value when  $\theta = 90^\circ$ , and  $\varphi = 90^\circ$  corresponds to the fact that when there is only a longitudinal component of the transmitting dipole, there is no  $H_T$  or  $H_L$  component of the magnetic field, as may be seen from the Table given above.

### **Analysis when the Angles of Elevation are no longer small**

In Part II of this article it was shown that when the angles of elevation at the receiver are no longer small, there are components  $H_L$  and  $E_L$  produced which are not due to the effect of earth losses, but to the actual inclinations of the wave fronts of the direct ray and the ray reflected at the surface of the earth. The problem has to be treated by the methods of geometrical optics, and in resolving the electric and magnetic fields in the direct and reflected waves along the  $T$ ,  $L$ , and  $V$  directions, account has to be taken of the polar diagram of the transmitting dipole regarded as a Hertzian oscillator. Expressions were given for the electric components, and it was shown that the longitudinal fields can be comparable with the transverse fields, and produce larger errors in the bearings which may vary considerably as the orientation of the transmitting dipole is altered, or the heights of the transmitter and receiver or the value of the wave-length are changed.

Similar expressions for the components of the magnetic field can be written down, and it can be seen that the errors when using the magnetic dipole (or vertical frame) under these conditions will be similar in kind, though differing from them in detail, to those obtained with the horizontal electric dipole. The same general remarks made in Part II therefore also apply to the case of the magnetic dipole, and we will not develop here the details of the analysis.

There is one aspect of the problem which has not been considered previously. It was assumed that the transmitter was a single dipole which could be resolved into three "in-phase" components. Actually, the three components may not be in phase, and the resulting polarization of the waves may not be plane but elliptical. In writing down the various components of  $E$  and  $H$  at the receiver, account must be taken of the differences in phase between the components of the transmitting aerial. At large angles of elevation, the modification will be one of detail in compounding the components of the fields, the general conclusions still holding. At small angles, the effect will be to modify the ratio and positions of the axes of the polarization ellipse.

### **Conclusions**

We have seen that although as a direction finder with ground waves the frame aerial becomes increasingly less subject to error, and the horizontal electric dipole more subject, as the wavelength is increased, on ultra-short waves, where the attenuation with distance is the same for both VED and VMD polarized waves, they behave in an analogous manner, and the general nature of the errors in bearing to be expected is similar for both types of receiving dipole. The order of the effects to be observed will be the same in both cases, though the detailed variations may be different.

The general conclusion is that both types of direction finder may be subject to large errors when the angles of elevation are large, and that when the distance is great enough to make these angles small, the goodness of bearing when the transmitter is well above the ground depends upon the magnitude of  $\frac{\lambda}{2\pi h_R}$  compared with unity.

When  $h_R$  is big enough to make  $\frac{\lambda}{2\pi h_R}$  very small, the bearing obtained should be reliable, apart from instrumental errors and the possible effects of local irregularities and site errors.

# WIDE-ANGLE SCANNING PERFORMANCE OF MIRROR AERIALS

J. F. RAMSAY, M.A., M.I.E.E. AND J. A. C. JACKSON

*Radar and radio frequently require wide-angle aerials where scanning or space diversity is obtained by feed displacement. The question of whether the aerial should be a lens or mirror then arises. This paper investigates experimentally the scanning realisable with a mirror. Two types of mirror were tested, viz. the coma-corrected zoned mirror, and the spherical mirror. With an offset feed, a line scan perpendicular to the offset can be obtained similar to that of a lens. The volume scan is, however, restricted if the offset feed is used.*

*Methods of assessing the available scanning in a given case are obtained from "scanning charts." It is shown how "pin-cushion" and "barrel" distortion can occur in microwave aerials as in optics.*

## Introduction

AS a guide to the possibilities of mirrors as scanning aerials an investigation was undertaken into the performance of two classical types, viz. the coma-corrected zoned mirror and the spherical mirror.

There existed at the time of the initiation of this investigation a certain lack of information (other than theoretical) on this subject. While lenses have been greatly favoured for the purpose and have many advantages, the reflector in some circumstances can be preferred. On axis a mirror aerial usually has higher gain than a lens. It is also likely to be less expensive, particularly as accurate radio mirrors can now be made.

The traditional electrical objections to mirrors, viz. reflection into and obscuration by the feed, are not always relevant. Vertex plate matching or offsetting will reduce reflection into the feed. Offsetting will also reduce obscuration. The mirror aerial only becomes difficult if such a large volume scan is required that the area of the feed involved leads to prohibitive obscuration.

While long focus, e.g.  $F = 1, 1.5$ , aerials are preferable for scanning, the mirror always has the advantage that some scanning is obtainable with short focus systems whereas short focus lenses are still at the problem stage, even on-axis.

The work was conducted at the 8-9 mm. or Q band. A suitable aperture diameter for the samples was taken to be 12 inch ( $35\lambda, 3^\circ$ , each with  $F = 1$ ).

## Design of a Coma-Corrected Zoned Paraboloidal Reflector

The polar equation of a paraboloid (Fig. 1) is

$$r = \frac{2f}{1 + \cos \Psi}$$

If the focal length is reduced in  $\lambda/2$  steps a family of confocal equiphase paraboloids is obtained given by

$$r = \frac{2(f - n \lambda/2)}{1 + \cos \Psi}$$

$$n = 0, 1, 2, 3, \dots$$

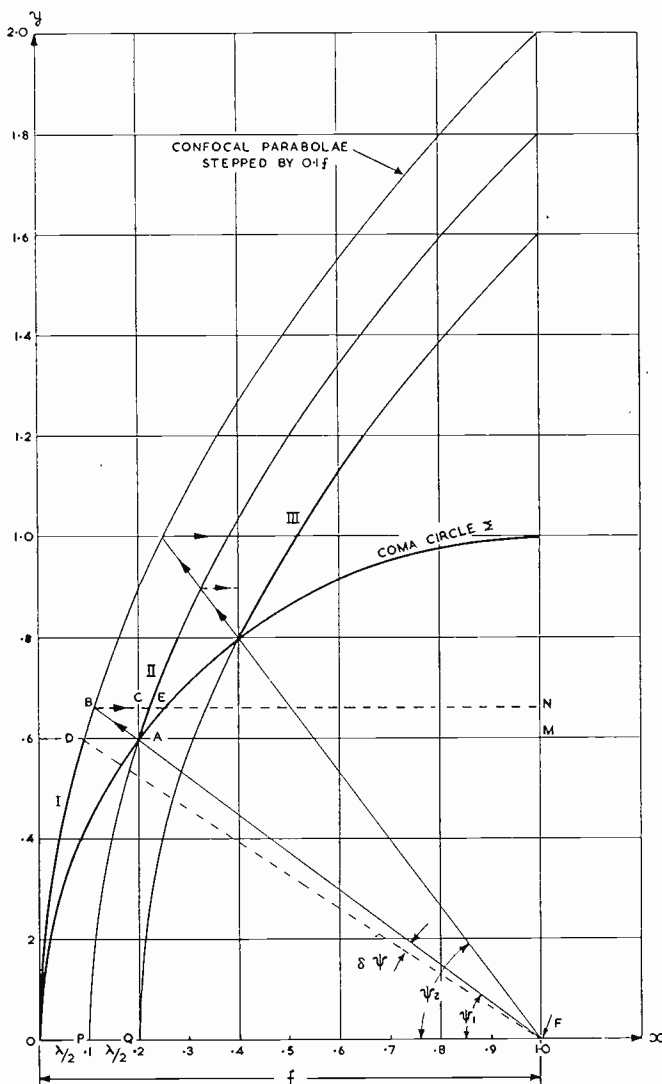


FIG. 1.  
Parabolae stepped to coma circle—general method.

$$FA + AM + \lambda = FA + AB + BC + CN$$

i.e.  $AB + BC = \lambda$

and the radial step is  $AB$ . There is however geometrical shadowing by  $AC$ . The

an equation defining a "stepped mirror."

For coma-correction the mirror has to be stepped to meet the coma circle  $r=f$ . If radial stepping is used such that the tips of the steps touch the coma circle the profiling takes the general form of Fig. 1, where  $F$  is the common focus.

The parabolae I, II, III are the first three members of the confocal set, corresponding to  $n=0, 1, 2$ . The focal step on the diagram is  $0.1f$ . For the equiphase condition this step is made equal to  $\lambda/2$ : then

$$FO + OF = FP + PF + \lambda = FQ + QF + 2\lambda$$

The coma circle has radius equal to the focal length  $f$ . The stepped mirror has to be profiled to this circle. In Fig. 1 the approximation to the profile has been obtained by making the tips of the steps lie on the coma circle. Thus the tip of the first step is where the parabola II intersects the coma circle. Then,

horizontal cut  $AD$  avoids the "shadow" but produces scattering. An intermediate or compromise cut could be used but due to the uncertainty of the regime in the step vicinity (partly geometrical-optical, partly diffraction), the practical cut  $AD$ , suited to ease of machining by turning on a lathe, has been preferred leading to cylindrical rather than conical steps.

The power in the solid angle represented by  $\delta\Psi$  is scattered. As the primary illumination is in general tapered in amplitude there will be an amplitude discontinuity at  $M$  in the aperture field distribution. If  $AB$  were the cut there would be a dip in the field between  $M$  and  $N$ . These are however geometrical descriptions. Due to the dimensions associated with the step being under the diffraction limit it is likely that these geometrical features are fogged by diffraction; and phase errors as well as amplitude irregularities are equally likely.

The tips of the steps in Fig. 1 are made to touch the coma circle. Instead, the middle of the steps could lie on the coma circle and give a better profiling approximation. It is evident from Fig. 1 that this closer approximation brings the zones closer to the axis, i.e. there are more steps. If the tips meet the coma circle the profiling is effectively to a circle of radius about  $f + \lambda/4$  and usually  $f \gg \lambda/4$  so that in most cases there is no disadvantage in "tip" approximations.

While Fig. 1 shows  $\lambda/2$  stepping,  $\lambda$  stepping can be used leading to fewer and deeper steps. In general any multiple of a halfwave may be used where necessary.

Since the point A lies on the coma circle  $r = f$  and on parabola II then

$$\frac{2\left(f - \frac{\lambda}{2}\right)}{1 + \cos \Psi_1} = f$$

$$\text{or } \cos \Psi_1 = 1 - \frac{\lambda}{f}$$

and the ordinate of A is given by

$$\begin{aligned} y_1 &= f \sin \Psi_1 = f \sqrt{1 - \left(1 - \frac{\lambda}{f}\right)^2} \\ &= \sqrt{2\lambda f - \lambda^2} \end{aligned}$$

The abscissa of A measured from the vertex is

$$x_1 = f - f \cos \Psi_1 = \lambda$$

Thus if the confocal family is given in cartesian form by

$$y^2 = 4 \left(f - n \frac{\lambda}{2}\right) \left(x - n \frac{\lambda}{2}\right)$$

the heights of the steps above the axis are obtained by putting

$$x_n = n\lambda, n = 1, 2, 3, \dots$$

That is, ordinates erected at  $\lambda$  intervals on the  $x$ -axis will intersect the coma circle  $r = f$  in the tips of the steps, a particularly simple construction.

The ordinates of the tips of the steps are given by

$$y_n^2 = 4 \left( f - n \frac{\lambda}{2} \right) n \frac{\lambda}{2}$$

$$= 2n \lambda \left( f - n \frac{\lambda}{2} \right)$$

For stepping through the tip parallel to the  $x$ -axis

$$y'_{n-1} = y_n$$

and abscissa of the intersection of the step with the  $(n-1)$ th parabola is given by

$$x'_{n-1} = (n-1) \frac{\lambda}{2} + n \frac{\lambda}{2} \left\{ \frac{f - n \frac{\lambda}{2}}{f - (n-1) \frac{\lambda}{2}} \right\}$$

The step depth is then

$$x_n - x'_{n-1} = (n+1) \frac{\lambda}{2} - n \frac{\lambda}{2} \left\{ \frac{f - n \frac{\lambda}{2}}{f - (n-1) \frac{\lambda}{2}} \right\}$$

$$= \frac{\lambda}{2} \left\{ \frac{1}{1 - \frac{n \lambda/2}{f + \lambda/2}} \right\}$$

from which it is observed that the step depth increases from  $\lambda/2$  on axis to deeper values as the zoning is extended off axis, as can be confirmed by referring to Fig. 1 which is drawn to scale.

This zoning technique may therefore be reduced to the following rules:

- (1) Find the tips of the steps by determining the intersections of the parallel lines  $x_n = n\lambda$  with the coma circle of radius equal to focal length. The heights off axis of the tips are then  $Y_n = \sqrt{\{2nf\lambda - n^2\lambda^2\}}$ .
- (2) Determine the steps by drawing lines through the tips of the steps parallel to the mirror axis, the depth of the steps so obtained being given by the intersection with the appropriate members of the family of parabolae, or without drawing the latter, by

$$\text{Step depth} = \frac{\lambda}{2} \left\{ \frac{1}{1 - \frac{n\lambda/2}{f + \lambda/2}} \right\}$$

It is of interest to record that a similar construction enables the stepping of a coma-corrected lens to be determined, e.g. the stepping of an eggbox lens having a spherical inner profile, the outer profiles being a family of stepped ellipsoids.

Thus both a coma-corrected mirror and a coma-corrected lens can be designed on the drawing board without computation; for the stepping can be obtained geometrically, and the depth of the steps is known, hence for all zones save the central zone linear (i.e. conical) approximations can be made by joining the root of one step to the tip of the next.

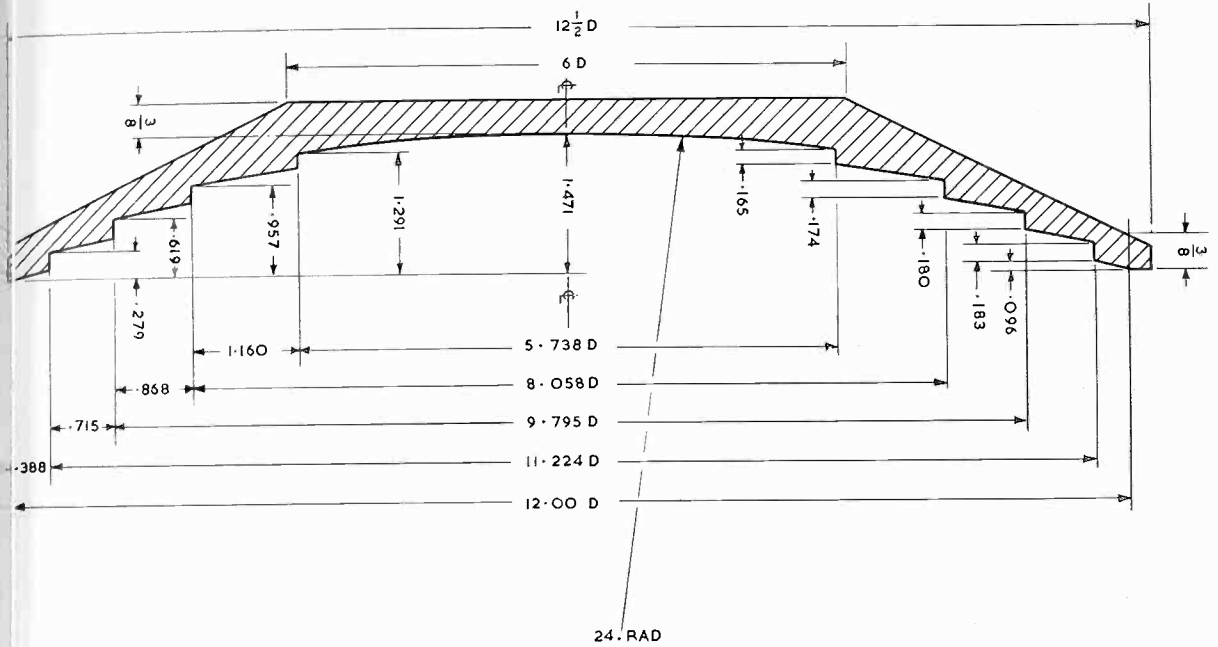


FIG. 2.

Section through centre line of 12 in. dia. zoned reflector ( $F=1$ ). (All dimensions in inches.)

The zeroth or central zone of the mirror can be made circular (i.e. rotationally spherical), with negligible error, of radius of curvature equal to twice the focal length.

The length of each tube on the central zone of an eggbox coma-corrected lens is given by

$$l = \frac{\delta}{1 - \mu}$$

where  $\delta$  is the phase error to be corrected at a height corresponding to the axis of the tube, and  $\mu$  is the index of refraction  $\lambda/\lambda_g$ ,  $\lambda_g$  being the wavelength in the tube. But for any point on the coma circle  $\delta$  is the length of the perpendicular from that point to the tangent through the origin, i.e. a geometrical length. Hence a linear subdivision of the first  $\lambda$  measured from the centre of the lens towards the focus will give, by erecting perpendiculars, a non-linear set of points on the  $y$  axis to which a linear set of tube lengths applies. Since however the tube spacing is regular, the inverse process must be used and the coma circle is divided equally by parallels to the  $x$ -axis. From the points obtained drop perpendiculars to subdivide the first  $\lambda$  of the  $x$ -axis non-linearly giving the quadratic phase errors corresponding to the points on the coma circle. From these intercepts the tube lengths are obtained from the formula  $l = \delta(1 - \mu)$ .

Even if these graphical methods suited to a drawing board are not used, e.g. because of inadequate accuracy, they portray the basic geometry and make any computation correspondingly easier.

In the particular zoned paraboloid made for the measurements and shown in profile section in Fig. 2 the radial step  $AB$  of theory was replaced not by  $AD$  but by  $BE$ , i.e. the tooth was removed rather than filled in. As is evident in Fig. 1 this lifts the tips of the practical steps away from the coma circle. On the scale of Fig. 2, however, where the aperture = focal length =  $35\lambda$  and  $\lambda/2 = .1715$  inch this lift is small and was tolerated as it allowed a slightly greater step height off axis.

The centre zone of the stepped mirror may be made spherical rather than paraboloidal owing to the closeness of the approximation involved. This subject is related to the second aerial studied viz. the spherical mirror, the design of which is discussed briefly in the following section.

### **Design of a Spherical Mirror Aerial.**

The spherical mirror scanning aerial is described by J. Ashmead and A. B. Pippard in the J.I.E.E. Vol. 93, Part IIIA, p. 627. "The Use of Spherical Reflectors as Microwave Scanning Aerials" a feature of this paper being the determination of the position of best focus. In optics, for paraxial rays, the focal length is half the radius of curvature. Ashmead and Pippard showed that a more precise position can be found given by

$$f = \frac{R}{2} - \frac{d}{4}$$

where  $R$  is the radius of curvature and  $d$  is the depth of the dish from the pole to the aperture plane. This position was calculated by assuming a paraboloid can be found having its vertex at the pole of the spherical mirror and its periphery coincident with the periphery of the spherical mirror. There is then some misphasing associated with the spherical mirror relative to the equiphase paraboloid; this the authors used as a general criterion for the spherical mirror aberration relative to a focus which is the focus of the paraboloid. The geometry of the relationship of the spherical mirror to the reference paraboloid and the deviation of the phase errors will be found in the paper. Due to phase errors the wave front has bulges in the direction of propagation.

The maximum phase error is approximately

$$\frac{2\pi}{\lambda} \Delta \max = \frac{2\pi}{\lambda} \frac{A^4}{2048f^3} = \frac{2\pi A}{\lambda \cdot 2048F^3}$$

so that if  $\Delta \max = \lambda/8$ , the available aperture is

$$A = 256 F^3 \lambda$$

where  $F = f/A$  is the  $F$  - number.

For the proposed aerial  $A = 35\lambda$ ,  $F = 1$  hence the maximum phase error on axis is.

$$\Delta \max = \lambda/60$$

This phase error is comparable with that resulting from constructional errors of profile, hence such an aerial approximates very closely to any practical paraboloid other than a purely optical mirror. The profile is not of course coma-corrected as in the case of a stepped mirror, hence some coma distortion would be anticipated.

## Wide-Angle Scanning Performance of Mirror Aerials

Astigmatism would be a major limitation in both types of mirror.

Some discussion of the off-axis performance of a spherical mirror will be found in the paper by Ashmead and Pippard. A theoretical derivation of the scanning locus and of the loss in gain on scanning is however still required.

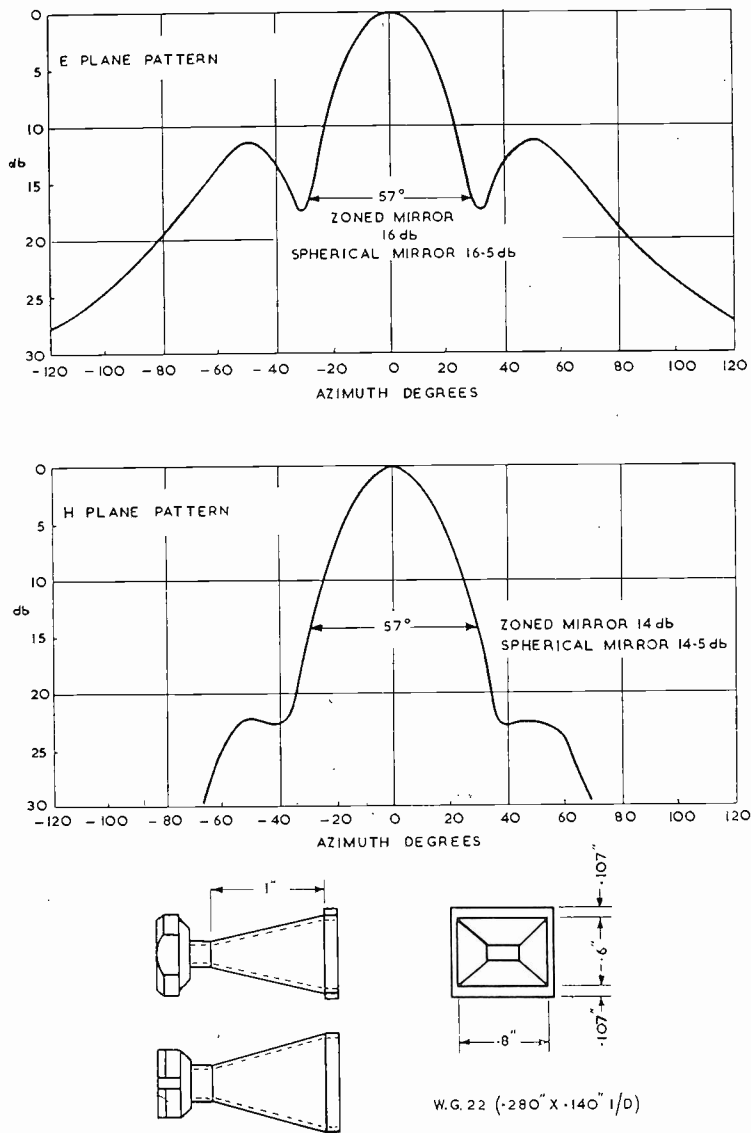


FIG. 3.

*Primary feed horn patterns and dimensions.*

Meantime the measurements of the performance described below indicate the performance that is realizable in a practical case. In the aerials a 15dB illumination taper was used and the feed horn always pointed at the centre of the objective.

The dimensions and principal plane patterns of the feed are shown in Fig. 3. This was an existing feed and was not specially developed.

**Performance of Coma-Corrected Zoned Mirror**

The mirror has a diameter of 12 inches, i.e. an aperture of  $35\lambda$  at 8.7 mm. (0.343 inches) wavelength. The focal length and the radius of the coma sphere were taken to be 12 inches for design purposes. The focus for maximum gain was found by measurement to be 12.35 inches, the range at which the determination was made being  $1.5 D^2/\lambda$  and the remote transmitter having an aperture of  $15.1\lambda$ . The true focus for infinite range is then 12.12 inches.

For the sake of record it is useful to have an estimate of the refocusing of a focused element at finite range. Using the lens equation as a first approximation

$$\frac{1}{v} + \frac{1}{u} = \frac{1}{f}$$

and taking the distance of the remote transmitter as  $u$  gives  $v$  the new focal length where

$$v = f + \Delta f$$

It is convenient to express the distance separating transmitter and receiver in Rayleigh Ranges, viz.  $k R_r$  where

$$R_r = \frac{1}{2} \frac{D^2}{\lambda}$$

$D$  being the aperture width of the receiving aerial under test.

Then

$$\frac{1}{f + \Delta f} + \frac{1}{k R_r} = \frac{1}{f}$$

Whence

$$\Delta f = \frac{f^2}{k R_r - f}$$

If  $f/D = F$  and  $R_r = 0.5 D^2/\lambda$

$$\begin{aligned} \Delta f &= \frac{F^2 D^2}{\frac{k}{2} \frac{D^2}{\lambda} - FD} \\ &= \frac{2F^2\lambda}{k} \left( 1 + \frac{2F^2\lambda}{kf} \right) \end{aligned}$$

At the Rayleigh Range  $k = 1$  and for  $F = 1, f = 35\lambda$

$$\Delta f = 2\lambda \left( 1 + \frac{2}{35} \right) = 2\lambda \times 1.057 = 2.114\lambda$$

For the range of the measurements  $k = 3$  hence

$$\Delta f = \frac{2}{3}\lambda \left( 1 + \frac{2}{105} \right) = 0.677\lambda = .23 \text{ inches.}$$

## Wide-Angle Scanning Performance of Mirror Aerials

No special care was taken to obtain the focus, the estimated accuracy being  $\pm \frac{1}{16}$  inch; this measurement should not be taken as accurate enough for long wave scaling.

The gain of a  $35\lambda$  circular aperture provided with constant illumination is 12,100, i.e. 40.8dB above an isotropic source.

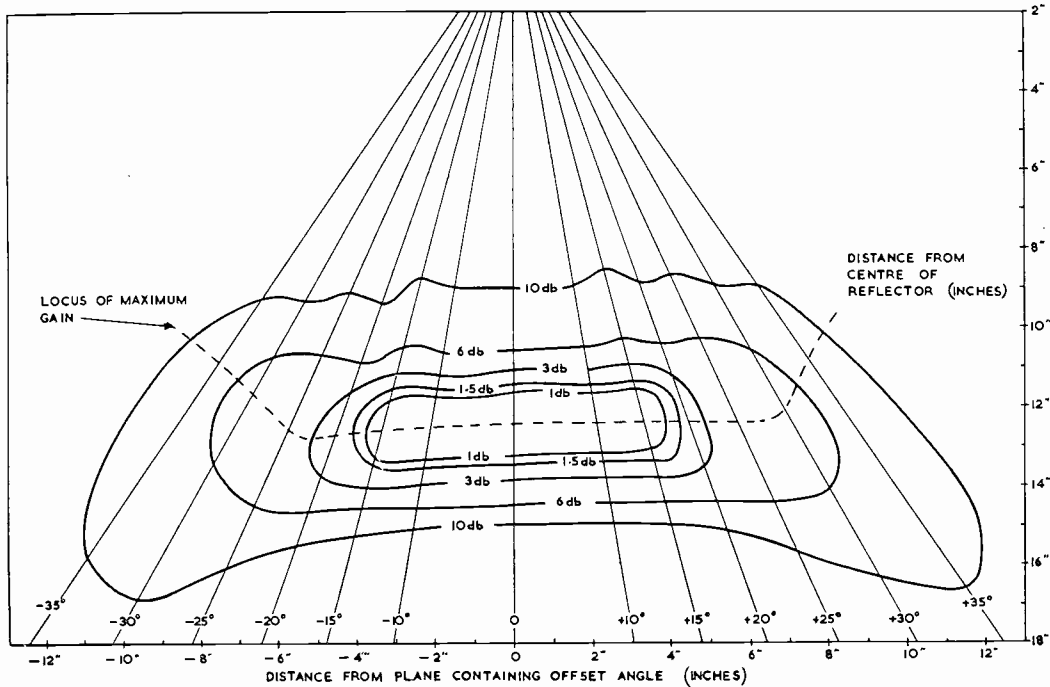


FIG. 4.  
Zoned mirror 12 in. dia.  $F=1$ . Isophote contours.

In the following gain figures which will be quoted the absolute accuracy is estimated to be within  $\pm 0.25$ dB the relative accuracy being about  $\pm 0.1$ dB.

The gain on axis at the measured focus was found to be 39.0dB by comparison with the measured gain 18.7dB of a standard pyramidal horn. That is, the loss of gain due to spillover, distribution and step discontinuities amounts to 1.8dB. This figure may be optimistic as it is close to the theoretical; or the step losses, conductivity, surface roughness, profile inaccuracy were not significantly affecting the loss. There were four steps; the material was aluminium alloy machined to profile. It is believed that the small steps of order  $\lambda/2$  and the reasonably well profiled dish contributed to maintaining the gain. It appears that these step, &c., losses are within the accuracy of measurement.

The performance of the mirror was required with the feed offset; for reference, the off-axis performance was first determined in the plane through the axis focus containing the centre of the mirror and perpendicular to the plane containing the proposed offset feed, that is, the wide angle scanning without offsetting.

Isophote contours, i.e. loci of constant gain for this plane are shown in Fig. 4. The curves were obtained by taking field measurements radially at different scan angles; the intensity of the maximum at any given scan angle was also measured

relative to the intensity at the focus. The contours are expressed in decibels relative to the intensity at the focus. These contours describe the depth of focus of the mirror over the scanning field and define the optimum scanning locus for maximum gain where the rate of change of slope is minimum.

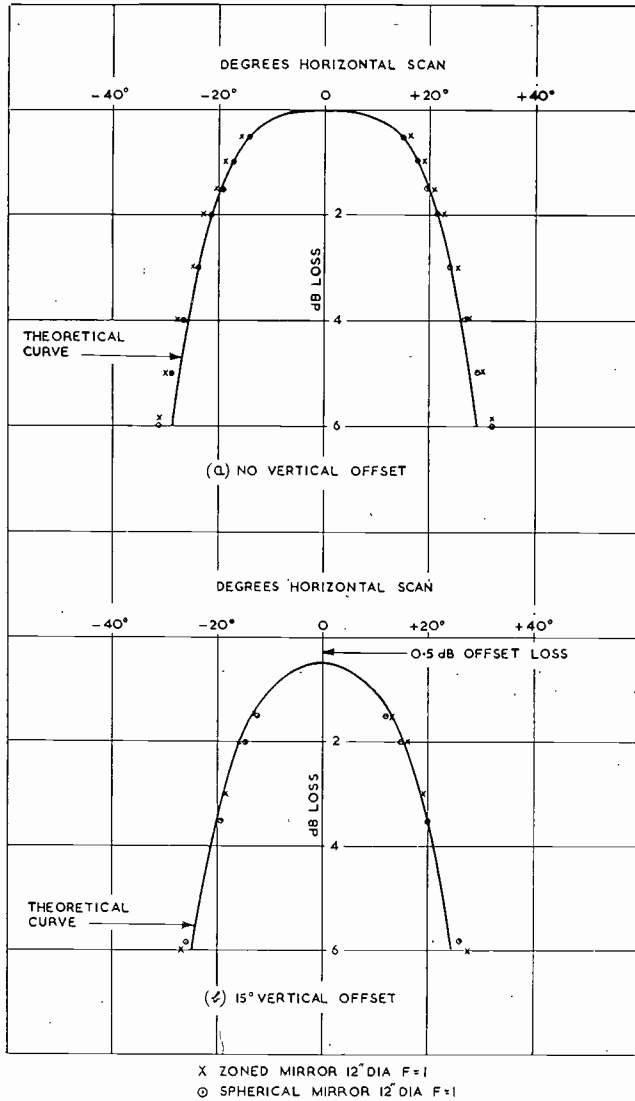


FIG. 5.  
 Loss of gain on scanning.

from the contours showing loss in gain versus scan angle (Fig. 5a). From the curve the loss in gain for an offset angle of 15° is 0.5dB.

When the feed is at the offset position any further feed movement in the same plane direction will give an elevation scan. If however the feed moves such that the

Because very often aerials are used beyond the Rayleigh limit of 1.5dB loss in gain, e.g. in height determination of aircraft, an attempt was made to plot the contours to as low a level as was consistent with an off-axis single focus being observable. While a 10dB contour is shown, its accuracy is doubtful. Satisfactory definition does not exist much beyond the 6dB level. While not a great deal of analysis was devoted to the diffuse behaviour around the 10dB level the curious distortion of contour encountered suggests beam asymmetry and splitting tendencies. Further measurements in these regions would be of value especially measurements of radiation patterns.

The equigain contours taken in a plane containing the focus determine the focal length of the dish.

The principal utility of this set of curves lies in its providing a representation of the field which gives both the shape of the optimum locus for off-axis scanning and the loss of gain on scanning with special reference to the offsetting requirement. As the loss in gain is particularly important a curve is derived

beam scans horizontally only from the initial offset position, a second set of contours can be obtained analogous to these of Fig. 4, where there was no offsetting. These contours, shown in Fig. 6 lie in a plane 30° below the horizontal plane.

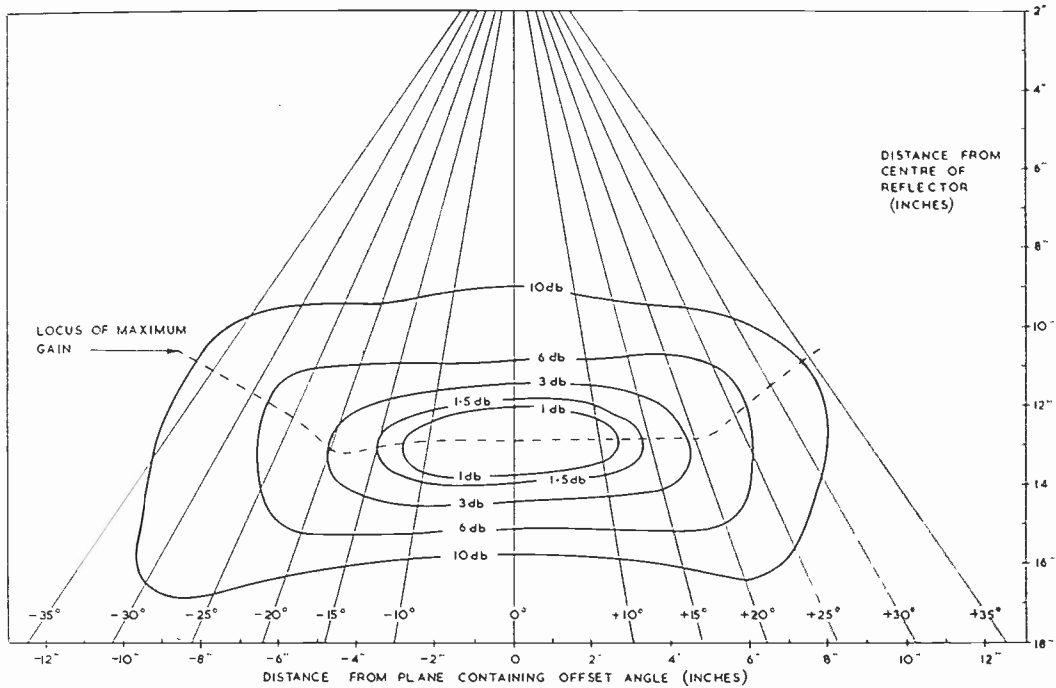


FIG. 6.

Scanning with offset feed of zoned mirror. 12 in. dia.  $F=1$ . Isophote contours.

These "offset" contours show the restricted field due to the offset; at very wide angle there is not very much difference as the losses are high there in either case, but the 1.5dB limit falls from  $\pm 20.5^\circ$  to  $\pm 13^\circ$ . This provides the scanning to the Rayleigh limit when the feed is always offset  $15^\circ$ . The scanning locus is closely linear. The corresponding curve for loss in gain on scanning when offset  $15^\circ$  is shown in Fig. 5b.

Similar contours could be taken corresponding to different elevation angles. However from the data so far obtained indications were that it would be unnecessary to measure these contours if a method could be obtained which provided the data for the offset case given the non-offset case. This method has been determined and is described in a separate article entitled "A Universal Scanning Curve for Coma Corrected Mirrors and Lenses." (To be published in the *Marconi Review*.)

Further discussion of the off-axis gain performance of the zoned mirror will be made later in this present report when the performance of the spherical mirror has been described.

The isophote contours of Figs. 4 and 6 enable "depth of focus" curves to be drawn, giving the variation of gain with axial (or radial) defocus; these are shown in

Fig. 7 where the depth of focus is shown before and after offsetting. The widths of these curves can then be empirically related to the widths of the focal spots for a 10dB tapered incident wave.

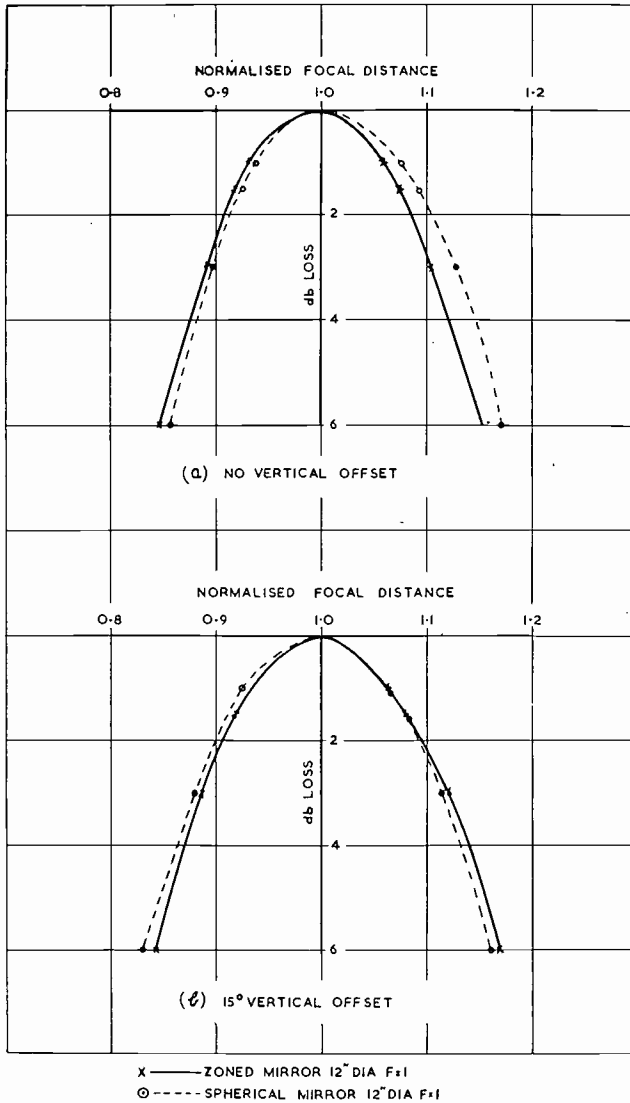


FIG. 7.  
Axial defocusing.

position 1 is 1dB. Both E and H plane patterns are shown in Fig. 9 for position 1 and 2.

It is to be observed that the lack of clear zeros on these patterns suggests the onset of astigmatism or the existence of a poor phase centre in the feed. The side-

This is shown in Fig. 8 when the ratio has been determined over the scanning field for levels of 3, 6 and 10dB. Thus at the 6dB level the depth of focus on axis is about 6.5 times the spot width. This provides a rough rule for relating axial defocus to beam width.

It will be observed in Figs. 4 and 6 that the feed locus for scanning with a coma-corrected zoned mirror is linear, the feed horn always pointing to the centre of the reflector. Beyond the 3dB level of loss in gain the locus becomes indistinct and concave towards the reflector.

The flat scanning field obtained with the coma-corrected zoned mirror is a distinguishing feature of this aerial.

### Radiation Patterns of the Offset Zoned Mirror

Radiation patterns were measured at the offset but not scanning position of the feed (position 1 in Fig. 3) and at the Rayleigh limit position when scanning horizontally. It should be observed that the 1.5dB loss includes the offset loss, and the pattern is taken at Position 2 where the loss in gain as compared with

Wide-Angle Scanning Performance of Mirror Aerials

lobe levels which are less than  $-20\text{dB}$  are of the order to be expected from the gain data.

At the scanning position some improvement is found indicating some unexplained compensating action.

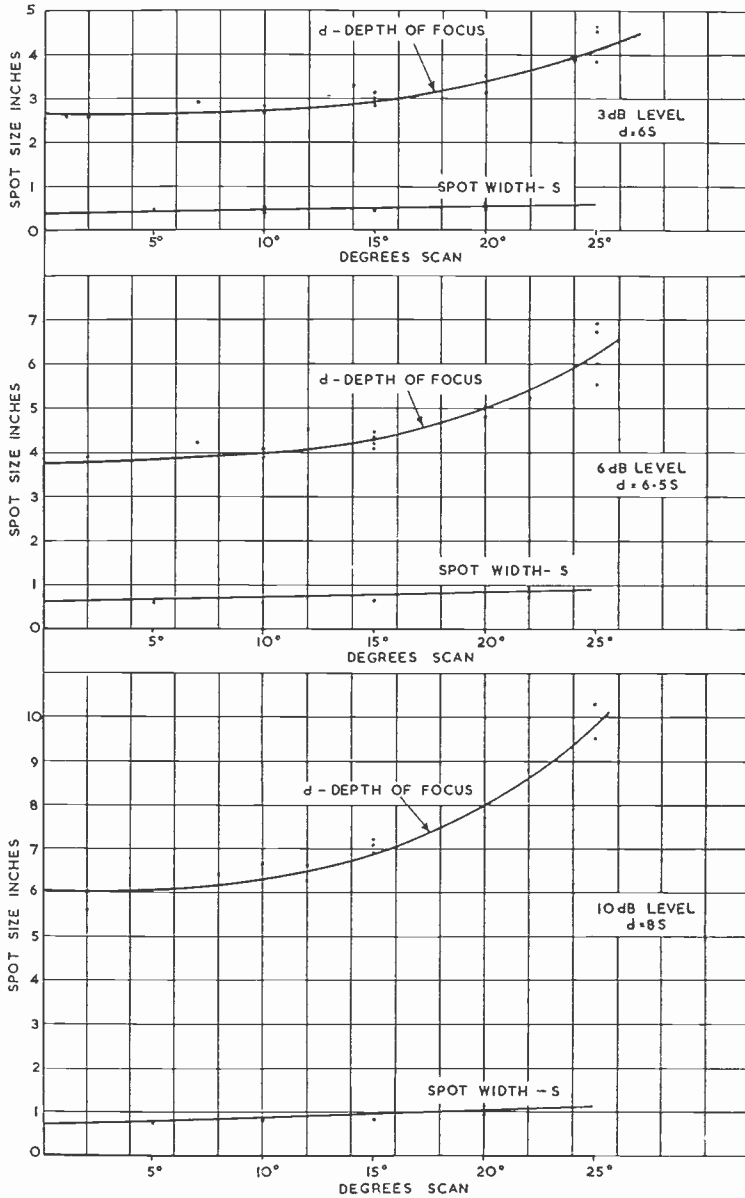


FIG. 8.  
Size of focal spot.

The beam widths yield a beam width factor between 102 and 108 for the two positions. The illumination taper is 15dB.

## Wide-Angle Scanning Performance of Mirror Aerials

The patterns of position 2 show a slight trace of asymmetry suggesting that the coma was not completely eliminated. It may have been due to the amplitude asymmetry. If coma exists, amplitude asymmetry has been found to exaggerate the pattern asymmetry.

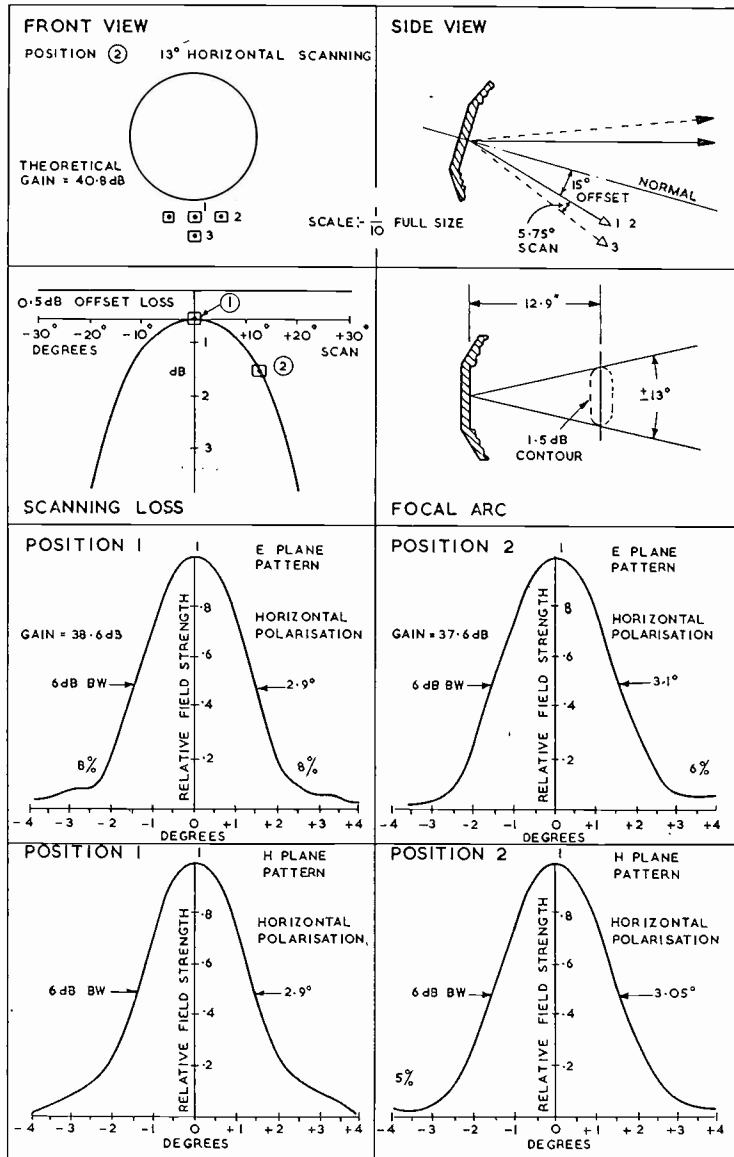


FIG. 9.

*Offset zoned mirror. 12 in. dia.  $F=1$ .  $\lambda=8.7$  mm.*

Radiation patterns for beam positions above the horizon were not recorded and would be of interest particularly at maximum scan angles. Preliminary information comparable to that obtained above was required for the spherical mirror aerial.

**Performance of Spherical Mirror**

The focus was determined by plotting isophotes for a scanning plane containing the axis of the mirror. The measured focal length is 11.75 inches, subtracting the refocusing correction of 0.23 inches then gives 11.52 inches. The theoretical focal length is 11.81 inches.

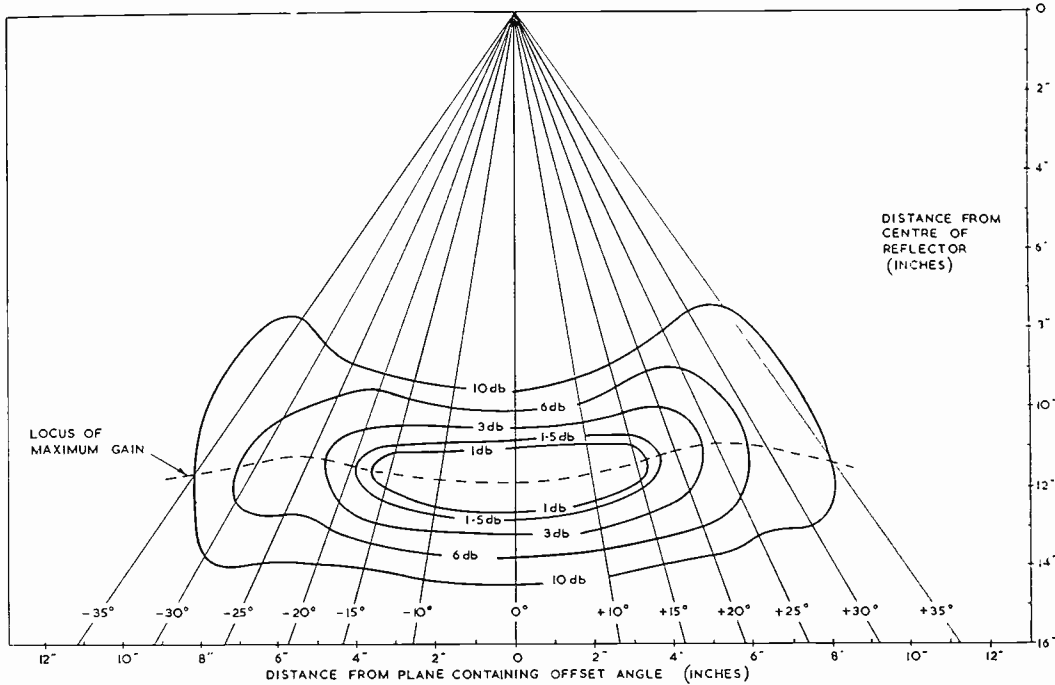


FIG. 10.  
Spherical mirror, 12 in. dia.  $F=1$ . Isophote contours.

From the isophote contours (Fig. 10) the optimum scanning locus is to a good approximation a sphere of radius equal to focal length. The field is therefore spherical.

The gain on axis was not worse than  $-2.2\text{dB}$  relative to that of constant illumination.

The loss in gain due to offsetting was  $0.5\text{dB}$ .

The scanning performance in a plane which is horizontal when the feed is offset is shown in Fig. 11 from which the limitation in scanning due to the offsetting will be evident.

The loss in gain on scanning without offsetting is shown in Fig. 5a, and with offsetting in Fig. 5b for comparison with the curves of the zoned mirror.

The depth of focus of the spherical mirror is also shown in Fig. 7 for comparison with that of the zoned mirror.

Some radiation patterns taken on the spherical mirror are shown in Fig. 12 and show low sidelobe levels. On scanning, however, pattern asymmetry develops. Further pattern information is still required.

**Comparison of Zoned Mirror with Spherical Mirror**

From the data obtained above the following comparison can be made between the coma-corrected zoned mirror and the spherical mirror.

## Wide-Angle Scanning Performance of Mirror Aerials

Item	ZM	SM	Notes
Loss in gain ... ..	Each $-2\text{dB} \pm .25\text{dB}$ (see Figs.)	$-2.5\text{dB}$	Feed on axis.
Loss in gain ... ..	$-2.5\text{dB}$ (i.e. $0.5\text{dB}$ offset loss)	$-2.5\text{dB}$	Feed offset.
Curvature of field ... ..	Plane	Spherical	$r = f.$
Half scan angle ... ..	$13^\circ$	$12^\circ$	For $-3.5\text{dB}$ total loss in gain.
Beam width (offset only) ... ..	$2.9^\circ$	$2.9^\circ$	$-6\text{dB}$ level.
Beam width (maximum scan) ... ..	$3.1^\circ$	$3.1^\circ$	$-6\text{dB}$ level.
Sidelobes (offset only) ... ..	$22\text{dB}$	$24\text{dB}$	
Sidelobes (maximum scan) ... ..	$25\text{dB}$	$24\text{dB}$	Some asymmetry.
Depth of focus (offset only) ... ..	$6.5$	$6.5$	Times (weighted) spot width at $-6\text{dB}$ level.

It may therefore be concluded that  $F=1$  coma corrected zoned mirrors and spherical mirrors have closely the same performance. The slight advantage of the zoned mirror is doubtful when the construction is taken into account.

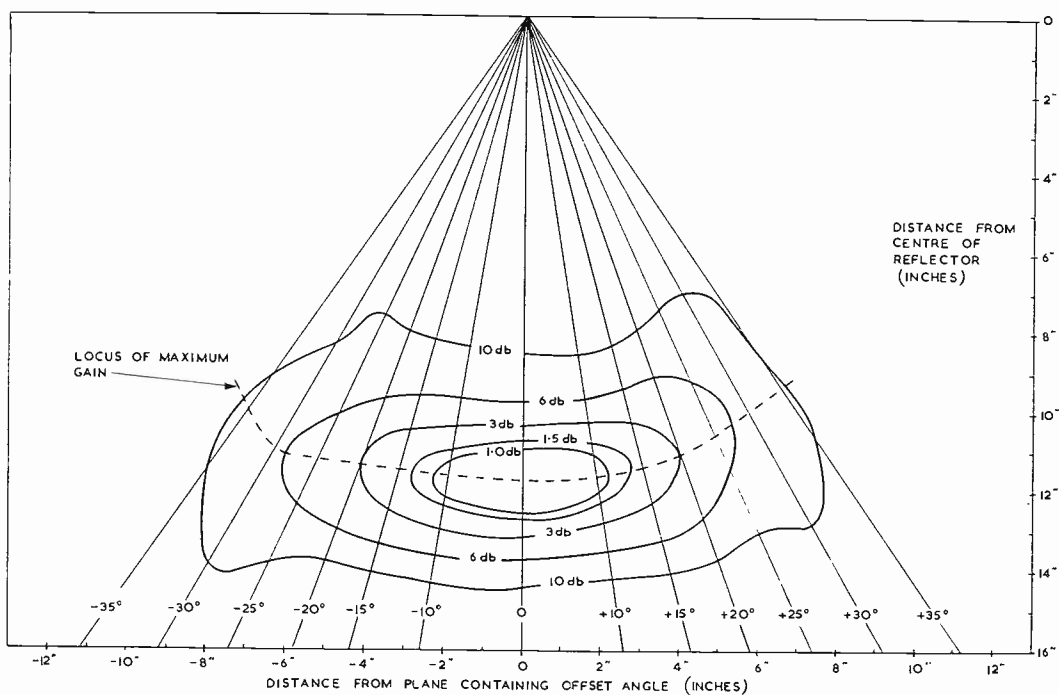


FIG. 11.

*Scanning with offset feed of spherical mirror. 12 in. dia.  $F=1$ . Isophote contours.*

The main feature of the investigation not yet mentioned is that the scanning performance of these aerials is almost identical with that of a coma-corrected lens of the same aperture. The absolute gain figures are of course superior to that of the average radio lens, by about 2dB.

Comparison of the Mirror Aerials with Lens Aerials

It is useful to compare the performance of the above orthodox mirror aerials with conventional coma corrected lenses. For convenience of reference the following notes have been drawn up.

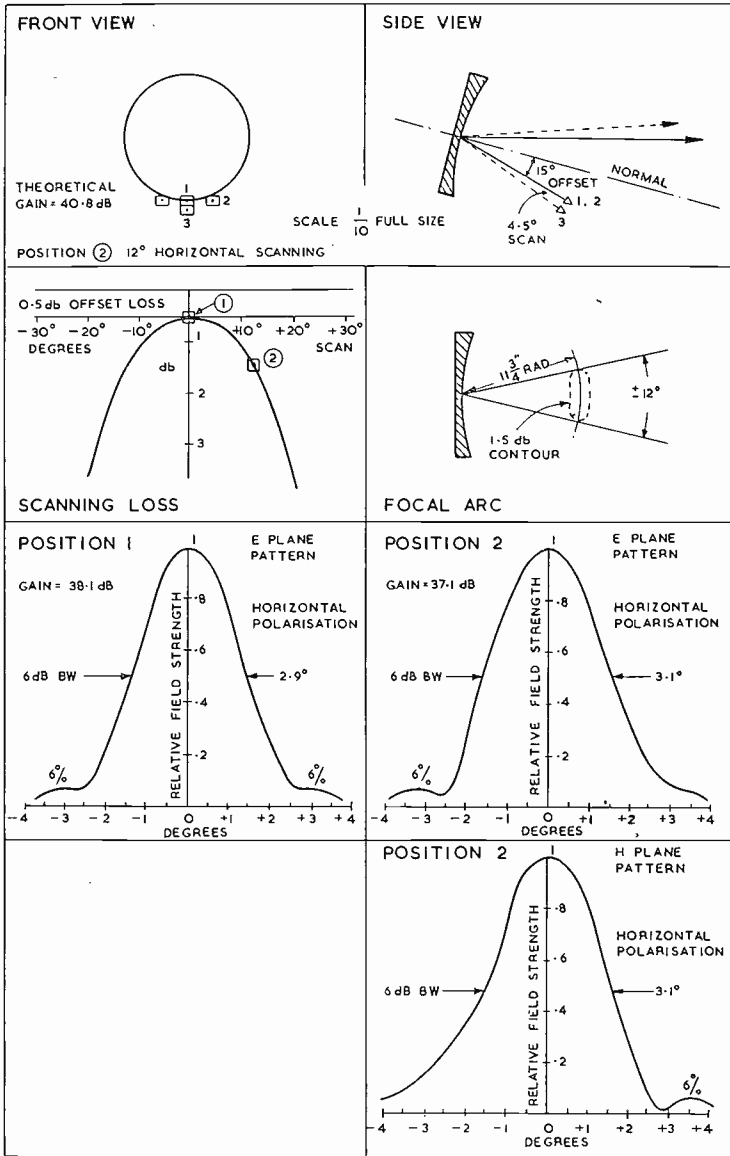


FIG. 12.

Offset spherical mirror. 12 in. dia.  $F=1$ .  $\lambda=8.7$  mm.

Gain

In most cases the on-course gain of a mirror aerial will be superior to that of a conventional lens even if an offset feed is used with a circularly symmetrical mirror.

### *Sidelobes*

The sidelobes on the radiation pattern of mirrors will be at least as small as, and frequently smaller, than that of a lens. Various situations arise (1) if the mirror aperture is very large and a single feed is used, not offset, the contribution of the feed to the sidelobe structure will be small, and the general sidelobe performances will be good, and better than that of a corresponding large lens. (2) If the feed is offset the sidelobe performance will be at its optimum. Both offsetting and low sidelobes are necessary for a multiple feed multi-beam aerial.

### *Scanning*

Because of their inferior gain figures lenses produce "weaker pictures" than mirrors. The *distribution* of intensity, i.e. loss in gain on scanning is the same, however, whether a lens or a mirror be used. Thus a project based on a lens could be replaced by a mirror and yield substantially the same volume of scan. If the mirror requires offset feeding then very limited scanning is obtainable in the plane of offset and the scanning perpendicular to the offset plane is somewhat less than that of a lens. Offset mirrors are essentially suited to giving a line scan rather than a volume scan.

### *Polarization*

The scanning performance of mirrors has been found to be substantially independent of polarization. With offset fed mirrors however, cross polarization is likely to be more evident than with lenses. It is important to review the polarization characteristics before making a choice.

### *Structural*

The design considerations are highly affected by the wavelength of operation. The following notes refer to the choice of aerials of lens or mirror type for S-band, and are based on current practice, rather than theory.

Although the interest in this paper is in scanning aerials, the scanning advantage is largely determined by profile, and the current construction of *non-scanning* aerials is not irrelevant. Non-scanning aerials are widely used, with aperture of the order required for radar, in microwave link communications. It is noteworthy that mirror aerials are much more popular than lenses. In links high gain, low sidelobes and pure polarization are also required. The two types of lenses used have been the metallic delay dielectric horn lenses of the Bell Telephone System in the U.S.A. and the perforated plate lenses in France.

The mirror type aerials have been centre fed paraboloids (U.S.A.) and horn-paraboloids (Bell System, Germany). The type of significance here is the offset-fed mirror, preferred because of the lack of reflection into the feed and the low sidelobes.

Offset fed reflectors have been made of metal, single skin or double skin with honeycomb filler; and fibreglass reinforced plastic. Metallized asbestos fibre has also been used.

Thus the accumulated experience in making large mirrors is to the advantage of the mirror as compared with the lens.

It would seem that when a line scan is required possibly with a small elevation scan the mirror is definitely preferable to the lens. When large volume scans are wanted artificial dielectric lenses represent the most likely focusing element provided the scanning is satisfactory; this is apparently still unexplored.

In the case of very large aerials where almost optical (telescope) designs can be used, the reflector may be preferable to the refractor as in optics.

#### *Cost*

Taking microwave links aerials as a guide, the windage and weight have to be a minimum if tower cost and therefore first order system cost have to be low. Aerial cost in itself has to be an absolute minimum. These considerations may indicate the basic preference for mirrors, leading to the conclusion that scanning mirrors are preferable to scanning lenses unless a large volume of scan is required.

#### **Scanning Charts. Pincushion and Barrel Distortion in Aerials**

In order to determine the scanning potentialities of an aerial at a glance it seemed worth while to portray the scanning field on a chart from which the performance could be read off. The method upon which a "scanning chart" is based is as follows: given an aerial of the focusing element type (lens or mirror with feed) a focal surface can be found which optimizes the gain at any angle of view. This surface is the "field" of an optical focusing element. The field is in general a curved surface. On the field surface contours can be drawn of equal (relative) gain. Usually these will be circularly symmetrical around the focus.

If these contours are then projected orthographically on to a plane through the focus and perpendicular to the axis of the focusing element, they will project, for a circularly symmetrical lens or mirror, as a set of concentric circles.

If on the field surface, angles of scan are marked, by associating with each feed position on the surface a specific direction in space, the field surface can be mapped in angular co-ordinates say azimuth and elevation. The map on the field surface thereby obtained can then be projected upon the tangential plane carrying the equi-gain circles.

A plane map is then obtained providing relative gain at any angle of scan, i.e. the scanning information required.

#### *The Zoned Reflector with a Flat Field Showing Pincushion Distortion*

Taking a wide angle scan through the focus gives as shown in Figs. 4 and 5, flat scanning locus and a loss in gain on scanning characteristic. Having established that these data are independent of polarization the field properties may be taken to have circular symmetry; hence the scanning locus is plane, i.e. the field is flat, and the loss contours are circles in that plane centred on the focus.

This type of aerial thus provides the basic field as aimed at in visible optics and automatically provides its own scanning chart as shown in Fig. 13. It may be pointed out that the "pincushion" distortion shown by the loci of constant azimuth and constant angles were obtained from experimental data before their theoretical justification was appreciated. Geographically speaking, the loci represent a gnomonic projection of two orthogonal sets of "meridians" and show the divergent feature of this projection, the curves being hyperbolae.

To the microwave aerial engineer the loci are significant in describing how a feed has to move or how multifeeds have to be distributed to yield radar scans of either constant azimuth angles or constant elevation angles as would be likely to be required in a practical case. Since the scanning movement is divergent this type of field is not the best. Obviously it has quasi-optical distortion.

For the present investigation however, the information gives the required scanning chart from which the available scanning of the aerial can be seen almost

## Wide-Angle Scanning Performance of Mirror Aerials

From the chart with the new scales, the performance of the other aerial is found.

For speed of reference it is best to read the scanning on the  $100\lambda$ , ( $1^\circ$ ),  $F = 1$  chart of Fig. 15, then multiply the half scan angle obtained by the factor  $\sqrt{\left(F \frac{100\lambda}{D}\right)}$  or  $\sqrt{(F \cdot BW)}$ .

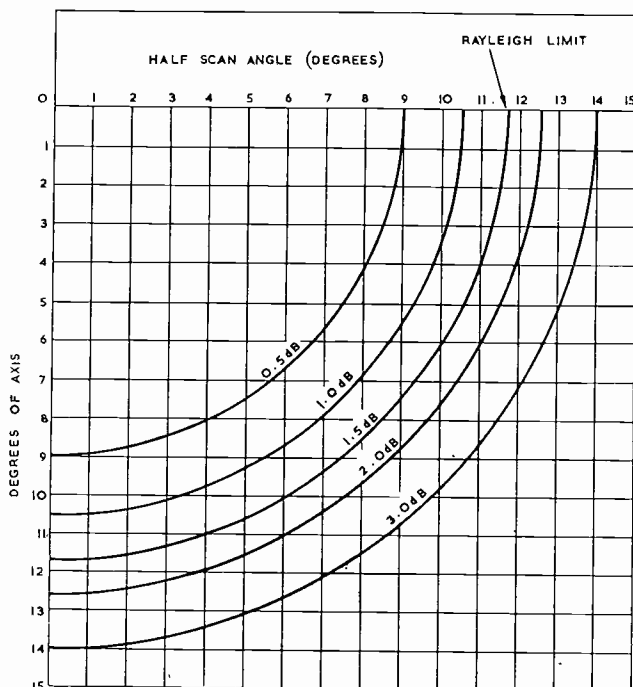


FIG. 15.

*Scanning chart for coma-corrected aerials.*

In the case of offset mirrors, when the aperture diameter (or beam-width) and  $F$  number are different from the normalized case, the offset angles ( $15^\circ$  for  $F = 1$ ,  $10^\circ$  for  $F = 1.5$ , etc.) are divided by  $\sqrt{\left(F \cdot \frac{100\lambda}{D}\right)}$  or  $\sqrt{(F \cdot BW)}$  before the normalized chart is used to determine the scanning available with an offset feed.

*Note.* While this report has been restricted to circular objectives the data obtained should indicate the wide angle scanning of elliptical objectives. It is evident for example that an offset elliptical reflector (offset in the direction of the minor axis) will give a two-dimensional scan superior to that of the circular mirror.

### Acknowledgements

Acknowledgement is made to the Board of Admiralty for permission to publish this paper. The authors wish to thank Mr. D. Roessler for suggesting the "isophote contour" measuring technique, and Mr. J. Chaplin for assisting in the work.

# MARCONI'S WIRELESS TELEGRAPH COMPANY, LIMITED

ASSOCIATED COMPANIES, REPRESENTATIVES AND AGENTS

- INDONESIA.** Yudo & Co., Djalan Pasar Minggu, 1A, Djakarta.
- IRAN.** Haig C. Galustian & Sons, Shahreza Avenue, Teheran.
- ISRAEL.** Middle East Mercantile Corpn., Ltd., 5, Levontin Street, Tel-Aviv.
- ITALY.** Marconi Italiana S.P.A., Via Corsica No. 21, Genova.
- JAMAICA.** The Wills Battery Co., Ltd., 2, King Street, Kingston.
- JAPAN.** Cornes & Co., Ltd., Maruzen Building, 6-2, Nihon-Bashidori, Chou-Ku, Tokyo.
- KUWAIT.** Gulf Trading & Refrigerating Co., Ltd., Kuwait, Arabia.
- LEBANON.** Mitchell Cotts & Co. (Middle East), Ltd., Kassatly Building, Rue Fakhry Bey, Beirut.
- LIBYA.** Mitchell Cotts & Co. (Libya), Ltd., Meiden Escuibada, Tripoli.
- MALTA.** Sphinx Trading Co., 57, Fleet Street, Gzira.
- MOZAMBIQUE.** E. Pinto Basto & Ca. Lda., 1 Avenida 24 de Julho, Lisbon. Sub-Agent: Entrepoto Commercial de Mocambique, African Life 3, Avenida Aguiar, Lourenco Marques.
- NETHERLANDS.** Algemene Nederlandse Radio Unie N.V.; Keizergracht 450, Amsterdam.
- NEW ZEALAND.** Amalgamated Wireless (Australasia), Ltd., Anvil House, 138 Wakefield Street, Wellington, C.I.
- NORWAY.** Norsk Marconikompani, 35 Munkedamsveien, Oslo.
- NYASALAND.** The London & Blantyre Supply Co., Ltd., Lontyre House, Victoria Avenue, Blantyre.
- PAKISTAN.** International Industries, Ltd., 1, West Wharf Road, Karachi.
- PANAMA.** Cia. Henriquez S.A., Avenida Bolivar No. 7.100, Colon.
- PARAGUAY.** Acel S.A., Oliva No. 87, Asuncion.
- PERU.** Milne & Co. S.A., Lima.
- PORTUGAL AND PORTUGUESE COLONIES.** E. Pinto Basto & Ca. Lda., 1, Avenida 24 de Julho, Lisbon.
- RHODESIA & NYASALAND.** Marconi's Wireless Telegraph Co., Ltd., Central Africa Regional Office, Century House, Baker Avenue, Salisbury.
- SALVADOR.** As for Guatemala.
- SAUDI ARABIA.** Mitchell Cotts & Co. (Sharqieh), Ltd., Jeddah.
- SINGAPORE.** Marconi's Wireless Telegraph Co., Ltd., Far East Regional Office, 35, Robinson Road, Singapore.
- SOMALILAND PROTECTORATE.** Mitchell Cotts (Red Sea), Ltd., Street No. 8, Berbera.
- SOUTH AFRICA.** Marconi (South Africa), Ltd., 321-4 Union Corporation Building, Marshall Street, Johannesburg.
- SPAIN AND SPANISH COLONIES.** Marconi Española S.A., Alcalá 45, Madrid.
- SUDAN.** Mitchell Cotts & Co. (Middle East), Ltd., Victoria Avenue, Khartoum.
- SWEDEN.** Svenska Radioaktiebolaget, Alstromergatan 12, Stockholm.
- SWITZERLAND.** Hasler S.A., Belpstrasse, Berne.
- SYRIA.** Levant Trading Co., 15-17, Barada Avenue, Damascus.
- THAILAND.** Yip in Tsoi & Co., Ltd., Bangkok.
- TRINIDAD.** Masons & Co., Ltd., Port-of-Spain.
- TURKEY.** G. & A. Baker, Ltd., Preuvayans Han, Tahtekale, Istanbul, and S. Soyal Han, Kat 2 Yenisehir, Ankara.
- URUGUAY.** Regusci & Voulminot, Avenida General Rondeau 2027, Montevideo.
- U.S.A.** Mr. J. S. V. Walton, 23-25 Beaver Street, New York City 4, N.Y.
- VENEZUELA.** English Electric de Venezuela C.A., Edificio Pan American, Avda. Urdaneta, Caracas.
- YUGOSLAVIA.** Standard, Terazije 20, Belgrade.
- YEMEN.** Mitchell Cotts & Co. (Middle East), Ltd., Victoria Avenue, Khartoum.
- YONKIN.** Mitchell Cotts & Co. (Middle East), Ltd., Victoria Avenue, Khartoum.
- ZAMBIA.** Mitchell Cotts & Co. (Middle East), Ltd., Kassatly Building, Rue Fakhry Bey, Beirut.
- ZANZIBAR.** Boustead & Clarke, Ltd., "Mansion House", Nairobi, Kenya Colony.
- AFRICA.** Sproston, Ltd., Lot 4, Board Street, Georgetown.
- WEST AFRICA.** (Gambia, Gold Coast, Sierra Leone.) Marconi's Wireless Telegraph Co., Ltd., West African Regional Office, 1 Victoria Street, Lagos, Nigeria. Sub-Office: Opera Building, Main Road, Accra, Gold Coast.
- ASIA.** Burmese Agencies, Ltd., 245-49, Suleia Road, Rangoon.
- AMERICA.** Canadian Marconi Co., Marconi Building, Trenton Avenue, Montreal 16.
- AMERICA.** Walker Sons & Co., Ltd., Main Street, Colombo.
- AMERICA.** Gibbs & Cia. S.A.C., Agustinas 1350, Santiago.
- AMERICA.** Industrias Colombo-Britanicas Ltda., Radio Colombiana De Seguros No. 10-01, Bogota.
- AMERICA.** Distribuidora, S.A., San Jose.
- AMERICA.** Audion Electro Acustica, Calzada 164, Casina A.L., Vedado-Habana.
- AMERICA.** S.A. Petrides & Son, Ltd., 63, Arsinoe Street, Nicosia.
- AMERICA.** Sophus Berendsen A/S, "Orstedhus", Farimagsgade 41, Copenhagen V.
- AMERICA.** Compania Pan Americana de Comercio, Boulevard 9 de Octubre 620, Guayaquil.
- AMERICA.** The Pharaonic Engineering & Industrial Co., 3, Sharia Orabi, Cairo.
- AMERICA.** Mitchell Cotts & Co. (Red Sea), Ltd., Martini 21-23, Asmara.
- AMERICA.** Mitchell Cotts & Co. (Red Sea), Ltd., Ababa.
- AMERICA.** S. H. Jakobsen, Radiohandil, Copenhagen.
- AMERICA.** Oy Mercantile A.B., Mannerheimvagen 12, Helsinki.
- AMERICA AND FRENCH COLONIES.** Compagnie Generale de Telegraphie sans Fil, 79, Boulevard de la Paix, Paris 8.
- AMERICA.** E. Pinto Basto & Ca. Lda., 1, Avenida 24 de Julho, Lisbon. Sub-Agent: M. S. B. Caculo, Cidade de Goa (Portuguese India).
- AMERICA.** P. C. Lycourezos, Ltd., Kanari Street 5, London.
- AMERICA.** Compania Distribuidora Kepaco, S.A., Avenida No. 20-06, Guatemala, C.A.
- AMERICA.** (Republic.) Maquinaria y Accesorios S.R.L., Tegucigalpa, D.C.
- AMERICA.** Marconi (China), Ltd., Queen's Road, Chater Road.
- AMERICA.** Orka H/F, Reykjavik.
- AMERICA.** Marconi's Wireless Telegraph Co., Ltd., "K" Block, Connaught Circus, Delhi.

